NAVAL POSTGRADUATE SCHOOL

MONTEREY, CALIFORNIA

THESIS

FINITE ELEMENT AND MOLECULAR DYNAMICS MODELING AND SIMULATION OF THERMAL PROPERTIES OF NANOCOMPOSITES

by

Daniel C. Kidd

June 2007

Thesis Advisor: Young Kwon

Approved for public release; distribution is unlimited

THIS PAGE INTENTIONALLY LEFT BLANK

REPORT DOCUMENTATION PAGE			Form Approved OMB No. 0704-0188
Public reporting burden for this collection of information is estimated to average 1 hour per response, including the time for reviewing instruction, searching existing data sources, gathering and maintaining the data needed, and completing and reviewing the collection of information. Send comments regarding this burden estimate or any other aspect of this collection of information, including suggestions for reducing this burden, to Washington headquarters Services, Directorate for Information Operations and Reports, 1215 Jefferson Davis Highway, Suite 1204, Arlington, VA 22202-4302, and to the Office of Management and Budget, Paperwork Reduction Project (0704-0188) Washington DC 20503.			
1. AGENCY USE ONLY ***(Leave blank)***	**2. REPORT DATE** June 2007	**3. REPORT TYPE AND DATES COVERED** Master's Thesis	
4. TITLE AND SUBTITLE Finite Element and Molecular Dynamics Modeling and Simulation of Thermal Properties of Nanocomposites			**5. FUNDING NUMBERS**
6. AUTHOR(S) Daniel C. Kidd			
7. PERFORMING ORGANIZATION NAME(S) AND ADDRESS(ES) Naval Postgraduate School Monterey, CA 93943-5000			**8. PERFORMING ORGANIZATION REPORT NUMBER**
9. SPONSORING /MONITORING AGENCY NAME(S) AND ADDRESS(ES) N/A			**10. SPONSORING/MONITORING AGENCY REPORT NUMBER**
11. SUPPLEMENTARY NOTES The views expressed in this thesis are those of the author and do not reflect the official policy or position of the Department of Defense or the U.S. Government.			
12a. DISTRIBUTION / AVAILABILITY STATEMENT Approved for public release; distribution is unlimited			**12b. DISTRIBUTION CODE**

13. ABSTRACT (maximum 200 words)

This study incorporated two approaches to determine the thermal conductivity of nanocomposite material using numerical modeling and simulation. The first was to look at the nanocomposite material at the macro level using a continuum model. The second approach broke the problem down to the atomic level and addressed the inter-atomic reactions using the Molecular Dynamics model.

The continuum model was used to determine the optimal placement and alignment of the nanoparticles within a nanocomposite, to provide the largest enhancement of thermal conductivity for the composite. During this process the effects of the particle size and spacing were investigated to determine the function that interparticle spacing and particle size plays in the thermal conductivity of the composite.

The Molecular Dynamics model was also used to calculate the thermal conductivity of nanocomposites given the thermal conductivity of the nanoparticles and the base material.

14. SUBJECT TERMS: Finite Element Method; Molecular Dynamics; Nanocomposites; Thermal Conductivity; Carbon Nanotubes, Nanoparticles			**15. NUMBER OF PAGES** 69
			16. PRICE CODE
17. SECURITY CLASSIFICATION OF REPORT Unclassified	**18. SECURITY CLASSIFICATION OF THIS PAGE** Unclassified	**19. SECURITY CLASSIFICATION OF ABSTRACT** Unclassified	**20. LIMITATION OF ABSTRACT** UL

NSN 7540-01-280-5500

Standard Form 298 (Rev. 2-89)
Prescribed by ANSI Std. 239-18

THIS PAGE INTENTIONALLY LEFT BLANK

Approved for public release; distribution is unlimited

FINITE ELEMENT AND MOLECULAR DYNAMICS MODELING AND SIMULATION OF THERMAL PROPERTIES OF NANOCOMPOSITES

Daniel C. Kidd
Lieutenant, United States Navy
B.S., The United States Naval Academy, 1998

Submitted in partial fulfillment of the
requirements for the degree of

MASTER OF SCIENCE IN MECHANICAL ENGINEERING

from the

NAVAL POSTGRADUATE SCHOOL
June 2007

Author: Daniel C. Kidd

Approved by: Young Kwon, PhD.
Thesis Advisor

Anthony Healey
Chairman, Department of Mechanical and Aeronautical Engineering

THIS PAGE INTENTIONALLY LEFT BLANK

ABSTRACT

This study incorporated two approaches to determine the thermal conductivity of nanocomposite material using numerical modeling and simulation. The first was to look at the nanocomposite material at the macro level using a continuum model. The second approach broke the problem down to the atomic level and addressed the inter-atomic reactions using the Molecular Dynamics model.

The continuum model was used to determine the optimal placement and alignment of the nanoparticles within a nanocomposite, to provide the largest enhancement of thermal conductivity for the composite. During this process the effects of the particle size and spacing were investigated to determine the function that interparticle spacing and particle size plays in the thermal conductivity of the composite.

The Molecular Dynamics model was also shown to calculate the thermal conductivity of nanocomposites given the thermal conductivity of the nanoparticles and the base material.

THIS PAGE INTENTIONALLY LEFT BLANK

TABLE OF CONTENTS

THIS PAGE INTENTIONALLY LEFT BLANK

LIST OF FIGURES

LIST OF TABLES

THIS PAGE INTENTIONALLY LEFT BLANK

ACKNOWLEDGMENTS

I would like to thank my thesis advisor Young Kwon for his guidance throughout this learning experience. Every meeting we had, invigorated me and motivated my excitement and interested in finding the answers and more of the questions. I would also like to thank my parents, Craig and Elizabeth Kidd, who I do not thank often enough for their guidance and sacrifices that supported me throughout my early years; and their continued support even now that I am older. Lastly I would like to thank my wife, Kimberly, without her love, support, and dedication to me and our children, this thesis and degree would never be possible.

THIS PAGE INTENTIONALLY LEFT BLANK

I. INTRODUCTION

A. JUSTIFICATION

The world of technology is becoming smaller and more powerful. Everywhere the hardware components are mimicking that trend; they are able to process more information at faster speeds. There is, however, a price to be paid to achieve the goal of the high power dense hardware components. The price is heat. The power used to process and operate cause the byproduct heat. Increasing temperatures in the components, without a means to dissipate this heat, will initially cause degradation and quickly lead to failure of the components and system.

The two modes of heat transfer that are typically used for cooling hardware are conduction and convection. Conduction is involved by transferring heat from the point of heat generation, within the component, to the housing or external part of the component. Convection (either forced or free) then transfers the heat from the outside of the component to a heat sink. A component that is more power dense does not have as much material and cooling area than that of a less power dense component. Less surface area may therefore reduce the efficiency of heat transfer. The overall effect is that the component will not cool sufficiently, then overheat, and ultimately fail.

The demand for more power dense hardware, therefore, will not be a viable reality without viable cooling techniques. There are different possible ways to address the cooling problem. The most general ways are to increase the cooling potential of either the conduction, or the convection modes. This thesis focuses on a method of using nanoparticles embedded into a base material to create a more thermally conductive nanocomposite material. This material will allow for greater heat dissipation from the point of generation to the convection interface.

The assumption, that nanoparticles such as Carbon Nanotubes (CNT) are much more conductive than the base material, leads to the hypothesis that the addition of a small amount of nanoparticles into the base material will have a great additive effect on the thermal conductivity of the entire composite material, thus increasing the heat flux through the material.

Similar assertions have been made and demonstrated using CNT to improve the strength and stiffness of composite materials. With as little as a one percent (by weight) of CNT dispersed into a composite material the stiffness increases between 36 and 42%; with a 25% increase in tensile strength. [1] It is reasonable to think that similar advances could be made to composite materials utilizing the thermal properties of the CNT.

Computer modeling and simulation will be used to numerically test this idea and to calculate quantitative results of thermal conductivity of the material. Previous experimental and theoretical work has been done to determine the true potential of nanocomposites' thermal properties. The studies have had mixed results. Past experimental results have been considerably higher than some older theories would have predicted. Analytic models have recently been offered to explain the conductivity of the CNT and how they react within a composite. These analytic models predict that the thermal conductivity of the composites can be much higher than the experimental data has shown.

The experimental work may be hampered by the delicacy of the CNT. Although they are very strong, because of their size they tend to intertwine with other tubes. It is also difficult to disperse, align, and orient the CNT throughout the composite to optimize their properties. Through computer modeling and simulation the alignment issues are eliminated; placement of the nanotubes can be specified throughout the composite, the spacing and orientation within the composite can be dictated to accurately determine how those variations will affect the thermal properties of the material. Models and simulations have limits

as well. The aim is to create and implement models that accurately mimic the conditions in a real system and are able to provide reasonable results with respect to the given loads.

B. OBJECTIVES

There are two goals of this thesis. First using numerical modeling and simulation to determine the optimal placement and alignment of the nanoparticles within a nanocomposite will be determined to provide the largest enhancement of thermal conductivity for the composite. During this process, the effects of the particle size and spacing will be investigated to determine the function that interparticle spacing and particle size plays in the thermal conductivity of the composite. Secondly a numerical model will be developed that will accurately calculate the thermal conductivity of nanocomposites given the thermal conductivity of the nanoparticles, and the base material and the volume fraction of the nanoparticles in the composite. Two independent models will be produced; a continuum model and a molecular dynamics model, to accomplish the first and second goals, respectively.

THIS PAGE INTENTIONALLY LEFT BLANK

II. BACKGROUND AND THEORY

This chapter will offer an overview of key components of the thesis. The first section will discuss nanoparticles, such as Carbon Nanotubes, and nanocomposites; whose properties are the primary, interest in this study. The theory of conduction, the heat transfer mode of interest, will be discussed in the second section. The other items covered in this chapter are the Continuum numerical method incorporating the Finite Element Method and lastly Molecular Dynamics. The continuum method and molecular dynamics are the basis for the models that are used to simulate the heat transfer through the nanocomposites.

A. THE CARBON NANOTUBE AND NANOCOMPOSITES

1. Carbon Nanotubes

The Carbon Nanotube (CNT) has been widely studied since the discovery in 1991. [2] The material properties are believed to be amazing; yield strength greater than that of high strength steels; thermal conductivity comparable that of diamonds (the most thermally conductive material known) [3]; excellent electrical conductivity. With those properties, the possible uses of the CNT seem to be unlimited, and new potential uses continue to propagate.

The Nanotube, as discovered by Iijima, is a seamless cylinder of graphite layers. Further work with the CNT has shown that the cylinders can be formed with fullerenes of carbon atoms capping the ends. The carbon atoms form a benzene-type hexagonal lattice to form the shell of the tube. They arrange in helical fashion around the tube's long axis of the tubes. [2] The tubes are approximately 2-10 nm in diameter (approximately 1/10,000 the diameter of a human hair) and have been grown as individual Single Walled Nanotube to four centimeters in length. [4]

Carbon based materials, in-plane pyrolytic graphite and diamonds, have the greatest measured thermal conductivity of any material at moderate temperatures. [5] The graphite cylinder that makes up the CNT have the same hexagonal molecular structure as that of the in-plane graphite sheets, Figure 1 illustrates this.

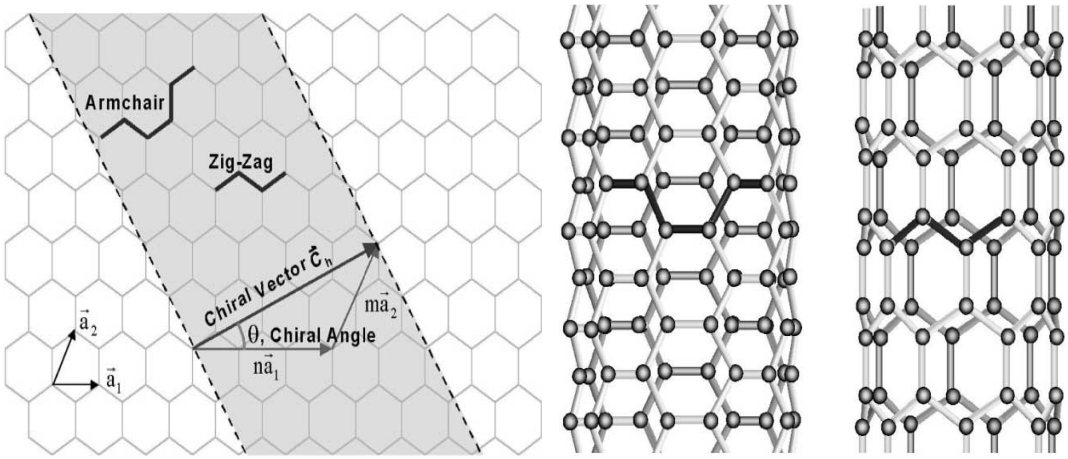

(a) (b)

Figure 1. (a) A schematic diagram showing how a hexagonal sheet of graphite is 'rolled' to form a CNT. (b) Illustrations of the two nanotube structures the Armchair and Zig-Zag from (a). [6]

Although the nanotubes are two dimensional, the extremely small diameter of the tubes reduces the dimensionality of the tube to practically one dimension. This graphite molecular structure and the small diameter suggest that CNT will have a thermal conductivity equivalent to that of diamonds. [7] The carbon make up of the nanotubes and the small size facilitate the phonon-phonon interaction in the axial direction of the CNT. The phonon-phonon interaction is a major factor in the heat conductivity of a material; this will be discussed further in the Conduction section of this report. Higher temperatures increase the phonon-phonon reaction, which is illustrated in Figure 2, as the thermal conductivity is a function of the temperature.

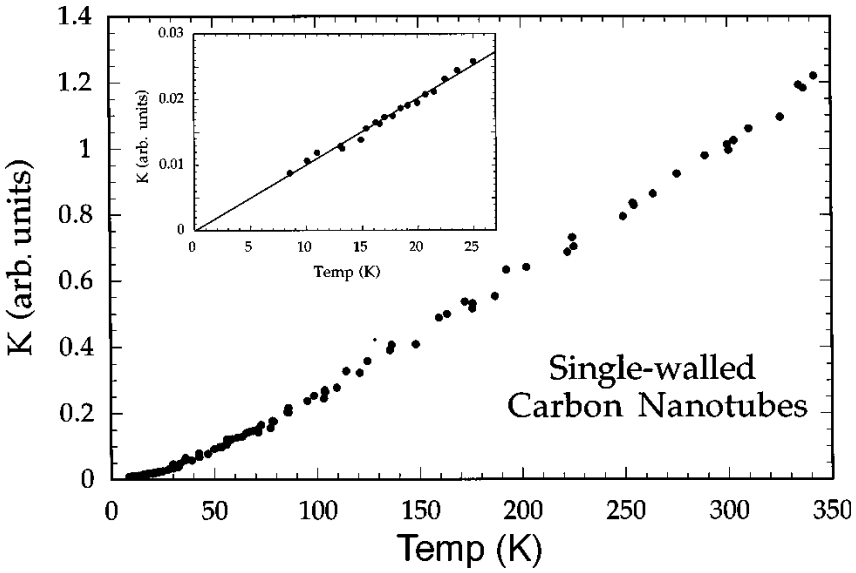

Figure 2. Thermal conductivity of SWNTs as a function of temperature. The inset highlights low temp behavior, the solid line is a linear fit for data below 25K. [8]

The CNT have been studied extensively, experimentally and numerically using Molecular Dynamics (MD). The results are almost as numerous as the studies. One MD study reported the thermal conductivity (κ) of a Single Walled Nanotube (SWNT) to be 2980 W/m-K. [9] A second MD study of an identical SWNT determined that κ = 6600 W/m-K (greater than that of a diamond). [10] Still other studies of using experimental approaches have estimated κ to range from 1750 to 5780 W/m-K for the SWNT. [8] Although there is a large range in the results for the thermal conductivity, there is a commonality that the results indicate that the CNT do have a high κ. The high thermal conductivity along with the other material properties ensures that there will be continued interest in developing CNT far into the future.

2. Nanocomposites

The nanocomposites are composite materials that typically have nanoparticles imbedded into their matrix; these particles are typically CNT but may be other nano-sized particles (for this report, the nanoparticles will be assumed in general). The initial focus on the work of nanocomposites was the hope of increasing material strength, which proved successful. More recently

there has been interest in the thermal advantages of nanocomposites. Most of the work has focused on the experimental results trying to measure the thermal conductivity of materials or creating analytical models that will accurately predict the composites' thermal conductivity. The results of these studies indicate that the maximum potential for the thermal conductivity of nanocomposites has not yet been achieved.

A 2001 experiment studied the thermal conductivity of oil with CNT in suspension. The results showed that with a 1.0 vol% of CNT in suspension a 1600% enhancement of the thermal conductivity was recorded. Previous theories of the conduction of fluids with particles in suspension predicted only a 10% increase in the conductivity. [11] The results of the 2001 study are shown below in Figure 3.

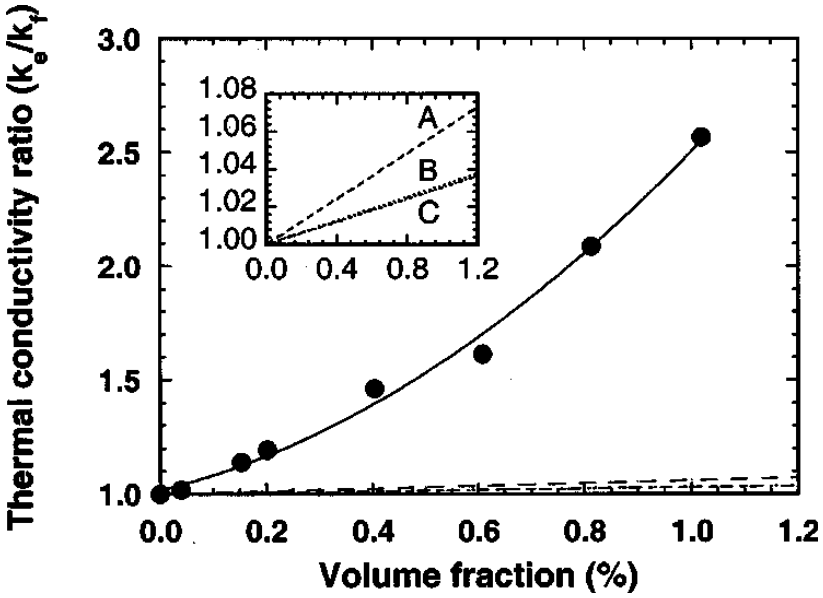

Figure 3. Solid dots represent the experimental results of the normalized conductivity data k_e/k_f (k_e is κ of the composite, k_f is κ of the fluid) CNT in oil suspension, compared to the dotted lines representing theoretical models for the enhancement of thermal conductivity in composite. κ ratio is 13800. [11]

The experimental results of solid nanocomposites in 2002 produced results of 125% thermal conductive enhancement through an epoxy composite

with 1 wt% CNT. This increase translated into $\kappa \cong 0.5$ W/m K; which was significantly lower than the researchers hoped to get according to the ”law of mixtures” prediction of 10W/m K. [12]

More recently however an analytic model has been developed to calculate the thermal conductivity enhancement of nanocomposites of randomly dispersed CNT throughout the composite.

$$\frac{\kappa_e}{\kappa_m} = \frac{3 + \frac{f\kappa_c}{\kappa_m}}{3 - 2f} \qquad (1)$$

κ_e : Thermal conductivity of the composite

κ_m : Thermal conductivity of the base material

κ_c : Thermal conductivity of the CNT

f : Volume fraction of CNT

For composite that have a small volume fraction of CNT (less than f =0.02) the expression for the enhancement becomes:

$$\frac{\kappa_e}{\kappa_m} = 1 + \frac{f\kappa_c}{3\kappa_m}. \qquad (2)$$

These analytic models were compared to the work done by Choi, Zhang, Yu, Lockwood, and Grulke in 2001. [13] Figure 4 shows this comparison, and also shows the disparity between the experimental and the analytical results.

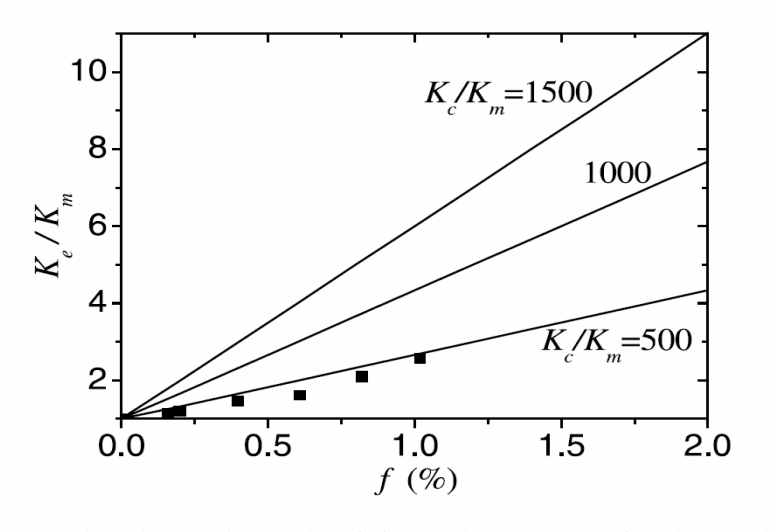

Figure 4. Solid Lines represent the thermal conduction enhancement using equation (2) compared to the experimental results (the solid dots) from reference. [14]

B. THE CONTINUUM METHOD (FINITE ELEMENT METHOD)

The Finite Element Method (FEM) is a numerical technique used to calculate and solve problems that do not have an analytical solution or that the system of interest is so complex that the analytic solution is too unwieldy to be used as a practical tool in solving the problem. An analytic solution provides the solution at an infinite number of points within the system; however, the FEM produces a solution at only a finite number of locations. Increasing number of location, referred to as nodes, in the system creates results that more closely match the analytic solution. The cost of this accuracy is the computing time associated with the calculations at each node.

The basis of the technique is to break the system up into a finite number of elements and then implement the boundary conditions and material properties for the system. The individual elements are modeled as homogeneous members. Therefore the solution across the well defined element is relatively easy to calculate.

The continuum computational process has been used in recent studies of carbon nanotube based composites. [15] Most of the work using the continuum

method and carbon nanotube based composites has been focused on the mechanical properties of the composites. It can, however, be assumed that these same techniques can be implemented to study the thermal properties of these emerging materials.

C. MOLECULAR DYNAMICS

The molecular dynamics approach is a simple one to grasp. It is, however, very challenging to implement. The premise is that the location of every body in a system is known at an initial time and the force on every body is also known. Then every future location, velocity, acceleration force and energy can be determined. The key is motion. The motion of molecules, regardless of whether they are solid, liquid, or gas molecules, is the important critical characteristic to determine all of the other values. The challenge of implementation is determining the exact initial conditions. The bodies in the system at the molecular level are enormous (there 6.022×10^{23} atoms per mole) and the time step size is incredibly small (the order of 10^{-15} seconds) to accurately calculate the atomic motion. These two parameters combine for an astronomical amount of computing power and time.

1. Classical Molecular Dynamics Method

The classical MD method is to calculate the position and velocities of all of the atoms as a function of time. The MD processor and solver are not concerned with the physical state (solid, liquid, gas) of the particular atom. The atoms are assigned an energy value, and it is this energy value that is the basis for the motion of the particle. At the atomic level, the atoms vibrate and move regardless of whether they are solid or fluid in nature. They will move more or less depending on the energy state of the atom. That being the case, it is a useful tool for modeling and simulating systems that containing multi-state and multi material systems. There are no issues or difficulties with modeling and analyzing of the interfaces between different states or materials, because the analysis is done at the atomic level. Using the atoms energy, Newton's second

law, Hamiltonian equation, and a potential energy function; the position and velocities of the atoms are calculated for a time step. The calculations are repeated for multiple time steps to calculate the solution.

The Quantum Molecular Dynamics model is another approach to the MD solution process. It is a model which is considered beneficial if the simulation and analysis is aimed at electron interaction between the atoms. The quantum MD model and simulation tend to be much more complex and more time consuming than that of the classical method, and as this work is not concerned with the electron interaction among the atoms the Classical MD approach was determined to be the correct choice. [16]

2. Newton-Hamiltonian Dynamics for the Classical Molecular Dynamics Simulation

When using the Newton-Hamiltonian Dynamics for MD simulation; the motion of the atom (*i*) is caused by force (F_i) exerted by an intermolecular potential energy (*U*). The motion of the atoms and applied forces are related through Newton's second law.

$$F_i = m\ddot{r}_i \tag{3}$$

Here *m* is the mass of the atom, independent of time and position. Acceleration ($\ddot{r}_i$) is represented by the equation:

$$\ddot{r}_i = \frac{d^2 r_i}{dt^2} \tag{4}$$

where r_i is the vector that gives the atom's position with respect to the coordinate system's origin. For a given N-atom system, Newton's second law represents 3N second order ordinary differential equation.

A conserved quantity in isolated systems is the total energy (*E*). It is possible to identify the total energy as the Hamiltonian (*H*). *H* takes the form of Equation (5); where *p* is the momentum of an atom and the potential energy *U* results from the interaction between atoms.

$$H(r^N, P^N) = \frac{1}{2m}\sum_i p_i^2 + U(r^N) = E \quad (5)$$

Taking the derivative of Equation (5) with respect to the distance *r*, the explicit relationship between the Hamiltonian and the potential energy is

$$\frac{\partial H}{\partial r_i} = \frac{\partial U}{\partial r_i}. \quad (6)$$

The resultant Hamilton's equations of motion are

$$\frac{\partial H}{\partial p_i} = \frac{p_i}{m} = \dot{r}_i \quad (7)$$

$$\frac{\partial H}{\partial r_i} = -p_i = -m\ddot{r}_i. \quad (8)$$

Using Equation (6) in the Equation (8) and comparing to Newton's Law (3) produces the equation.

$$F_i = -\frac{\partial H}{\partial r_i} = -\frac{\partial U}{\partial r_i}. \quad (9)$$

Any conservative force can be written as the negative gradient of some potential energy function U, and the forces from all of the other atoms determine the acceleration of each atom in the given system. [17]

3. Molecular Dynamics Soft Sphere (MDSS)

The most important aspects of a classical MD code are the applied potential energy functions and the finite difference method that is used. There are two main categories for the pair potential energy functions as they relate to the classic MD codes. They are the soft sphere potential and the hard sphere; the soft sphere potential represents the continuous energy function with respect to the inter-atomic distance, while the hard sphere potential represent a discontinuous energy function. The soft sphere approach is used for this thesis.

MDSS simulations codes tend to use a Verlet type algorithm or Predictor-corrector algorithm as the finite difference method to numerically solve the

differential equations of motion. These algorithms are usually chosen over the Euler or the Euler-Cromer based algorithms, because the Euler and Euler-Cromer tend to have numerical errors that are too big to tolerate at the small scales that MD operates at. [16]

The MDSS code used for this thesis was originally developed by J.M. Haile. [17] His code incorporates the Lennard Jones Potential (Equation (10)), as the potential energy function, and uses Gear's Predictor-Corrector Algorithm to calculate the motion of the atoms.

$$u(r) = 4\varepsilon[(\frac{\sigma}{r})^{12} - (\frac{\sigma}{r})^{6}] \qquad (10)$$

Gear's Predictor-Corrector Algorithm:

Prediction: A fifth order Taylor series to describe the atoms position at $t + \Delta t$ based on the position and the derivatives at time *t.*

$$r_i(t+\Delta t) = r_i(t) + \dot{r}_i\Delta t + \ddot{r}_i(t)\frac{(\Delta t)^2}{2!} + \dddot{r}_i(t)\frac{(\Delta t)^3}{3!} + r_i^{iv}(t)\frac{(\Delta t)^4}{4!} + r_i^{v}(t)\frac{(\Delta t)^5}{5!} \qquad (11)$$

$$\dot{r}_i(t+\Delta t) = \dot{r}(t) + \ddot{r}_i\Delta t + \dddot{r}_i(t)\frac{(\Delta t)^2}{2!} + r_i^{iv}(t)\frac{(\Delta t)^3}{3!} + r_i^{v}(t)\frac{(\Delta t)^4}{4!} \qquad (12)$$

$$\ddot{r}_i(t+\Delta t) = \ddot{r}_i(t) + \dddot{r}_i\Delta t + r_i^{iv}{}_i(t)\frac{(\Delta t)^2}{2!} + r_i^{v}(t)\frac{(\Delta t)^3}{3!} \qquad (13)$$

$$\dddot{r}_i\ (t+\Delta t) = \dddot{r}_i(t) + r_i^{iv}\Delta t + r_i^{v}{}_i(t)\frac{(\Delta t)^2}{2!} \qquad (14)$$

$$r_i^{iv}(t+\Delta t) = r_i^{iv}(t) + r_i^{v}\Delta t \qquad (15)$$

$$r_i^{v}(t+\Delta t) = r_i^{v}(t) \qquad (16)$$

Evaluation: Intermolecular Force on each atom is calculated at $t + \Delta t$.

$$F_i = -\sum_{j\neq i}\frac{\partial u(r_{ij})}{\partial r_{ij}}\hat{r}_{ij} \qquad (17)$$

Correction: Equations 18-23 offer the correction factors for the positions and their derivatives for the difference between the evaluated force and the predicted acceleration.

$$r_i = r_i^P + \alpha_0 \frac{\Delta\ddot{r}_i(\Delta t)^2}{2!} \tag{18}$$

$$\dot{r}_i = \dot{r}_i^P \Delta t + \alpha_1 \frac{\Delta\ddot{r}_i(\Delta t)^2}{2!} \tag{19}$$

$$\frac{\ddot{r}_i(\Delta t)^2}{2!} = \frac{\ddot{r}_i^P(\Delta t)^2}{2!} + \alpha_2 \frac{\Delta\ddot{r}_i(\Delta t)^2}{2!} \tag{20}$$

$$\frac{\dddot{r}_i(\Delta t)^3}{3!} = \frac{\dddot{r}_i^P(\Delta t)^3}{3!} + \alpha_3 \frac{\Delta\ddot{r}_i(\Delta t)^2}{2!} \tag{21}$$

$$\frac{r_i^{iv}(\Delta t)^4}{4!} = \frac{r_i^{(iv)P}(\Delta t)^4}{4!} + \alpha_4 \frac{\Delta\ddot{r}_i(\Delta t)^2}{2!} \tag{22}$$

$$\frac{r_i^{v}(\Delta t)^5}{5!} = \frac{r_i^{(v)P}(\Delta t)^5}{5!} + \alpha_5 \frac{\Delta\ddot{r}_i(\Delta t)^2}{2!} \tag{23}$$

D. CONDUCTION

Conduction is one of the three modes of heat transfer, the transfer of heat energy through contact. This thesis is investigating the heat transfer through the nanocomposite material, not the heat transfer to the environment, thus conduction is the focus for the study. The heat transfer modeled and simulated in this thesis is conduction heat being transferred from one boundary of the solid composite material one dimensionally to another boundary at steady state conditions.

Conduction is governed by Fourier's Law of Conduction.

$$q'' = -\kappa(i\frac{\partial T}{\partial x} + j\frac{\partial T}{\partial y} + k\frac{\partial T}{\partial z}) \tag{24}$$

Heat flux (*q"*) is a directional quantity. When the heat flow is restricted to one direction, as are the continuum models of this thesis dealt, call it the *x* direction; equation (24) is simplified to

$$q'' = -\kappa * \frac{\Delta T}{\Delta x}. \qquad (25)$$

Rewritten, to solve for the conduction coefficient, as

$$-\kappa = \frac{q'' * \Delta x}{\Delta T}. \qquad (26)$$

Δx : Length of the direction of the heat flow

ΔT : Temperature difference on the boundaries

q": Heat flux

κ : Thermal Conductivity Coefficient

It is interesting to note that Fourier's law was not developed from first principles; rather it was developed by Fourier from observed phenomena. Therefore the law is considered phenomenological, and a generalization based on immense amounts of experimental data. [18] The thermal conductivities of most engineering materials have been well documented and tabulated; κ values are historically based on the experimental data. Objects or components that are made of more than one tabulated material or composites that do not have a well documented thermal conductivity may be described by a modified, or hybrid, κ value known as the effective thermal conductivity (κ_{eff}). Substituting κ_{eff} into equation (26)

$$-\kappa_{eff} = \frac{q'' * L}{\Delta T}. \qquad (27)$$

This κ_{eff} term will be the primary result that the numerical models will be calculating.

The thermal conductivity coefficient, also known as the transport property, is a property of the material that varies with the state and the temperature of the

material. In solids it is an additive function of two phenomena of atomic interaction, the electron interaction and secondly the lattice vibrations, known as phonons. Solids tend to have a higher transport property than fluids, because the atoms are more closely packed and the electron and phonon activity more easily moves between atoms. The thermal conductivity coefficient in solids is described as

$$\kappa = \kappa_e + \kappa_l \tag{28}$$

$$\kappa_l = \sum_p C_p v_p l_p \,. \tag{29}$$

κ_e is the electron interaction component and κ_l is the lattice component. κ_l is a function of *C, v, and l* (the heat capacity, phonon group velocity, and the mean free path of the phonon of mode *p*). [19] In metals and materials of low electrical resistance the κ_e term is usually much larger and tends to dominate equation (28). [18] Although, it has been shown that in CNT this is not the case as seen in references [7, 8] that the phonon-phonon interaction, or κ_l, within CNT is the significant term in Equation (28). This phonon-phonon interaction validates the decision to use the Classical MD simulation opposed to the Quantum MD simulation, which is more useful when describing the electron movement between atoms.

THIS PAGE INTENTIONALLY LEFT BLANK

III. MODELING

The nanocomposite will be modeled in two distinct manners. First using the continuum method, this is a large scale view of the nanocomposite material and how it will transfer heat under simulated load situations. The continuum method uses the Finite Element Method (FEM) to calculate the heat flux across the nanocomposite. Since the heat flux is a function of the dimensions of the material, κ_{eff} for the material is calculated value that will be used for comparison of composite materials.

Molecular Dynamics is the second modeling technique that will be used in this study. The Molecular Dynamics (MD) approach calculates the average thermal conductivity of the atoms by using the data of the interaction between atoms at the atomic level.

A. CONTINUUM METHOD

The continuum models were created and run using the ANSYS 10.0 University Advanced software package for pre and post processing. The composite material was modeled as a two dimensional rectangular plate, and the nanoparticles were represented as areas within the plate boundaries. During the process of testing and analysis the shape of the nanoparticles were varied as rectangles, circles, and as hexagons to determine the effect on the κ_{eff}. The results from these different shapes will be discussed during the results chapter later in this paper.

1. Pre-processing

a. Settings and Boundary Conditions in ANSYS

The Thermal Preference in ANSYS was selected which activates the capability to solve thermal dynamic scenarios, create thermal boundaries, and enables the user to select elements designed to process thermal calculations. The element type used for all of the models, in the continuum

simulations, is *Thermal Mass, Solid, Quad 4node 55*. Each plate was modeled with a constant temperature on the left and right boundaries, 100 and 0 respectively. The top and bottom boundaries were modeled with a boundary condition of zero heat flux to indicate insulated boundaries. These boundary conditions were imposed to limit the heat flow to the *x*, or horizontal, direction.

b. Meshing

The circular shaped particles were meshed using the *Smart Size function level 5*. When the particles were modeled as the other shapes (rectangles and hexagon), they were meshed by dictating the element size on each line of the particle. This was typically an element length of 0.01 units. However, on the long boundaries of the rectangular particles, an element length of 0.1 was used.

The primary concern for the meshing of the remainder of the plate was to have specified element length on the temperature boundaries. This requirement was so that the distance between the nodes was known and the nodal heat flux could be numerically integrated. The decision on the size of the element length required a balance of accuracy, computational time, and data processing capability. The initial intent was to have all the same element length for every element on the boundary. This was not always practical. It was desirable to have a very fine mesh in the sections of the boundary that were influenced by the heat flux of the nanoparticle. The boundary sections of the plates that were not influenced by the higher thermal conductive particles did not require a fine mesh. As the mesh size got smaller, the computational time was longer as was the post-processing time, without any increase in accuracy for the results. The plate boundary mesh became a hybrid of element sizes. Sections of the boundary, influenced by the higher conductive particles, had a finer mesh; the other sections had larger element sizes. The small element length was modeled as 0.01 units and the larger element lengths 0.1.

2. Processing and Post-processing

The following ANSYS settings were used for the solution processing of the steady state response to the thermal boundary conditions. *Steady State* was chosen as the *Analysis Type*. ANSYS version 10.0 allows the user to choose from 1-5 for the computational speed under the menu; *Fast Solution Options* one being the fastest calculation speed and five being the slowest but most accurate speed. The simulations' results for this thesis were calculated using the slowest most accurate computational speed setting. Accuracy was more desirable than time efficiency for this study.

The post processing and data analysis was a three step process. The nodal heat flux data (q''_{nodal}) from the ANSYS output file was exported to an Excel spreadsheet. The q''_{nodal} was extracted for the nodes identified on the right hand boundary. The conservation of heat dictates that the heat flux through any *x* location on the plate should be equal to every other *x* location. With that information the post processing time can be reduced by only evaluating the nodes along a vertical boundary. This data was numerically integrated using the trapezoidal rule to calculate the total heat flux for the plate at the boundary. The average heat flux per unit length and κ_{eff} for the plates are derived from the total heat flux. The effective thermal conductivity was normalized (κ^*_{eff}) with κ_{eff} of an isotropic plate of the same dimensions. The value of κ^*_{eff} is used to compare the composite plates to determine the most effective heat transfer material.

B. MOLECULAR DYNAMICS

The Classical MD simulation process was used in this thesis to calculate the κ_{eff} of the nanocomposite material. The MATLAB software package was used to model and process the molecular dynamics model. The code *mdss_gp* [20] and its associated subroutines were originally written in FORTRAN and created by J.M. Haile [17] as *mdss* (Molecular Dynamics Soft Sphere). This code was developed originally to simulate Argon atoms using the Lennard-Jones potential as a soft sphere. The *mdss* code, and the subroutine codes, were

reformatted and modified into MATLAB code by Young Kwon into *mdss_gp* to calculate thermal conductivity in carbon nanotubes as well as polymers and metallic materials; then modified further for this thesis to calculate the thermal conductivity of a Face Centered Cubic (FCC) solid. The *mdss_gp* obtains the atomic positions of the FCC atomic positions. These atomic locations were produced by a subroutine code *create_fcc.* The *create_fcc* code produced a text file *input1.txt* that the *mdss_gp* file accessed to begin the calculations

The nanocomposite material was again modeled to determine the thermal conduction coefficient, this time modeling using the molecular dynamics method. The material was modeled as a Face Centered Cubic (FCC) molecular distribution of atomic positions, using *create_fcc* MATLAB code. [21]

The initial step was to calculate the heat conduction of an isotropic material at various energy (epsilon) and sigma values. Sigma represents the distance to Zero in the Lennard-Jones Potential, and Epsilon is the depth of minimum in the Lennard-Jones Potential. The actual values of epsilon, sigma, mass, and other properties within the MD code were arbitrary and used to model different materials to facilitate the simulation. The heat conduction values of the isotropic materials were compared to determine which primary and secondary materials could be used to create suitable κ ratios within a composite material. The desired κ ratios were to be similar to those in the continuum models. After the epsilon and sigma values for the primary and secondary materials were determined the composite material was modeled with in the MD code.

The isotropic FCC structure was converted to a composite material by changing the epsilon or sigma values of selected atomic positions within the cubic structure to the corresponding values of a material with a higher κ value (secondary material). The remainder of the atomic positions retained the values for the material with a lower κ value (primary material). This created particle locations within the FCC structure that had higher thermal conductivity than the

rest of the solid. The nanocomposite now modeled, κ_{eff} for the entire composite FCC structure could be calculated using the MATLAB *mdss_gp* code. The following geometries were tested:

- MD Model 1 Two groups of nine atoms. The two groups are separated in the x-direction, but fall in the same range of Y and Z values. The volume fraction of the more conductive atoms to the lower is 7.03%. Figure(5)
- MD Model 2 Two groups of 18 atoms. The two groups are separated in the x-direction, but fall in the same range of Y and Z values. The volume fraction of the more conductive atoms to the lower is 14.06%.
- MD Model 3 One section of 16 atoms that run the x-length of the cube. The volume fraction is 6.25%. (Figure 6)
- MD Model 4 One section of 32 atoms that run the x-length of the cube. The volume fraction is 12.5%.

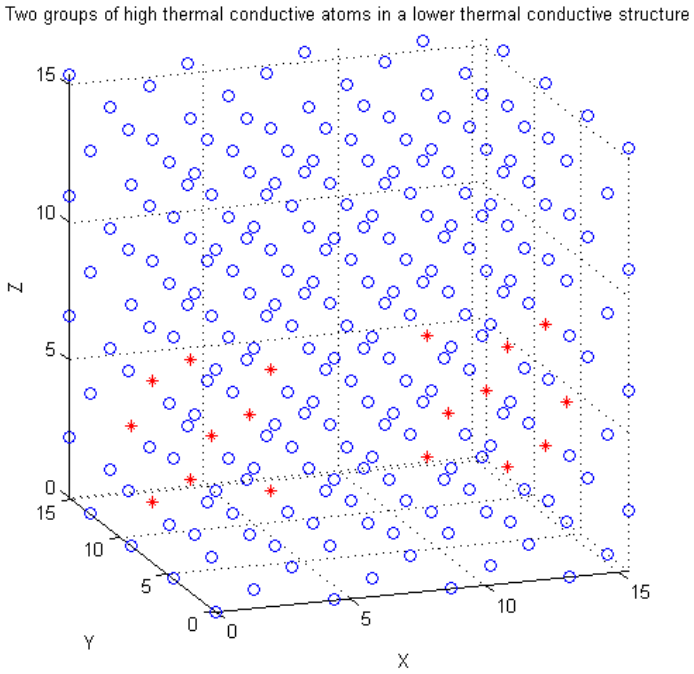

Figure 5. FCC structure of the primary material with two groups of atoms of a secondary material imbedded in the solid. The secondary material atoms are the red asterisk.

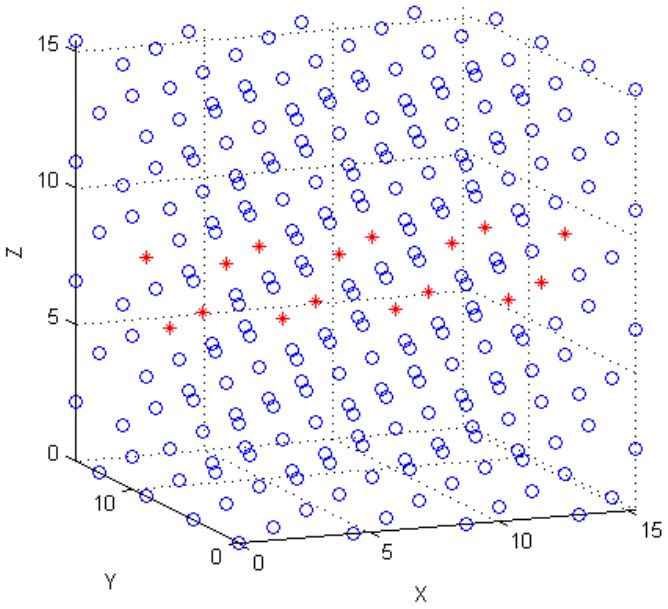

Figure 6. FCC structure of the primary material with a continuous section of secondary material the entire x-dimension of the structure. The atoms of the secondary material are indicated by the red asterisk.

Many combinations of epsilon and sigma were tested to determine a high and low value for sigma, which would produce a desired κ ratio for the nanocomposite ratios while epsilon was kept constant. These test combinations produced isotropic materials that would be used as the primary and secondary materials in the models. The heat conductivity of the isotropic FCC materials is listed in Table 1. The material with the lower value of sigma corresponds to the lower heat conductivity. The κ ratio of the primary and secondary material is approximately $5x10^4$ for the constant epsilon materials. The materials with the higher κ are used as the secondary materials in the MD models.

	epsilon	sigma	heat conductivity
Primary Material	1	2.4	9.67E-01
Secondary Material	1	4	4.91E+04

Table 1. The Heat Conductivity of the primary and secondary materials used in the MD models and the associated Sigma values.

IV. RESULTS AND DISCUSSION

A. CONTINUUM METHOD

Equation (27) becomes Equation (30) by replacing κ_{eff} with a normalized value of κ_{eff} (κ^*_{eff}), and ΔT =100. The *L* term varies with the plate dimensions; and *q"* is calculated with ANSYS 5.1.

$$-\kappa^*_{eff} = \frac{q"^* L}{100} \qquad (30)$$

1. Low Volume Fraction Models

The first plates to be modeled and tested were five by five plates with imbedded secondary particles. The models had very low secondary material volume fraction, and the particles were spaced as evenly as possible throughout the primary plate. The volume fractions ranged between 0.06-1.01% with spacing of 10 to 20 times the diameter of the particles. Even at a κ ratio of 10,000 there was very little change (less than 0.5%) in the thermal conductivity of the composite plate. These results indicated that a larger volume fraction was needed to see any significant results. The plate was modeled with the secondary material 10% of the volume of the plate. The step from 1% to 10% volume fraction is a large step and was done to ensure that that there would be a noticeable effect on κ_{eff}, after which the volume fraction could be adjusted to more realistic amounts.

2. Ten Percent Volume Fraction

a. Eight Particles

The increase to 10% had the desired effect. Incorporating eight particles into the 5x5 plate caused a sizable increase in κ_{eff} for the plate. In the initial distribution of eight particles the particles were spaced evenly throughout the plate shown in Figure 7.

The finite element plot from this simulation showed that the nodes on the y-boundaries that were inline with the particles from the top and bottom rows (three particles in a horizontal line) had a greater heat flux than those associated with the particles that were farther apart. Figure 8 is a line graph of the nodal heat flux values superimposed onto the FEM contour plot to illustrate this point. This result led to the question of whether the boundary heat flux was influenced more by the percentage of the boundary that was affected by the higher heat flux through the more conductive particles, or was the intensity of the heat flux at the boundary a greater influence. That is, is it better to align the same number of particles in fewer rows, or is better to spread the particles across the plate in the *y* direction.

A new geometry was modeled to determine if the intensity was the greater influence. Using the same eight particles in two horizontal lines (Figures 9 and 10). The continuity of the higher thermal conductivity did translate to a greater overall heat flux and κ_{eff} for the entire plate, Figure 11 shows this comparison. It is difficult to quantitatively compare the amount of boundary area affected by the higher thermal conductive particles; all of the nodes register some increase of heat flux over the nodes of an isotropic plate. Comparing the nodal heat flux of the top and bottom corners of the Figure 7 geometry to the corresponding nodes in the two row geometry a simple comparison is made. The nodal heat flux at the upper and lower corners of the three row plate's boundary are noticeably higher than the corresponding nodes in the two row geometry. This shows that the heat flux is spread out over more of the boundary area in the three row geometry. The thermal conductive enhancement from Figure 7 to Figure 10 is not very large (around 2-3% increase); however it shows a trend that needed to be further investigated.

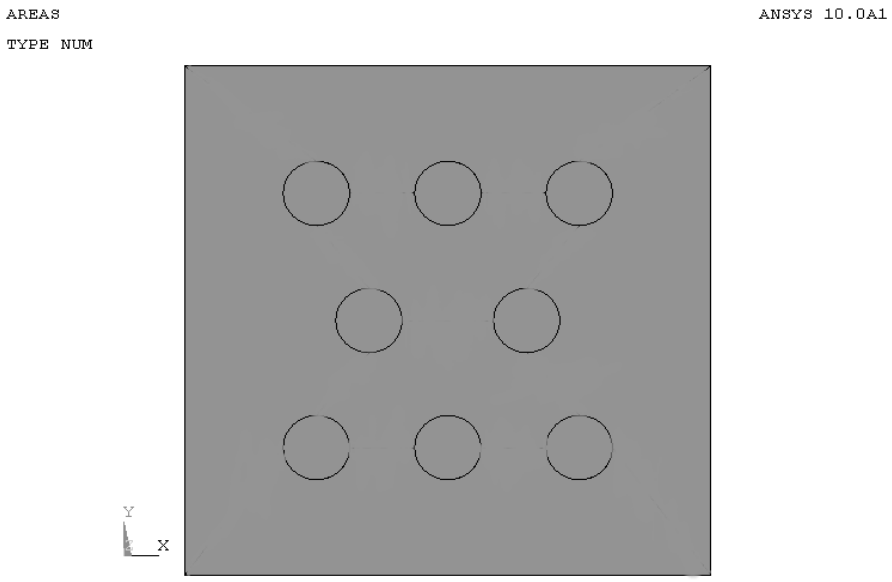

Figure 7. Eight particles (evenly spaced) diameter 0.6308, a 10% volume fraction. Dimensions of the plate are 5 in the *x*-direction 5 in the *y*-direction.

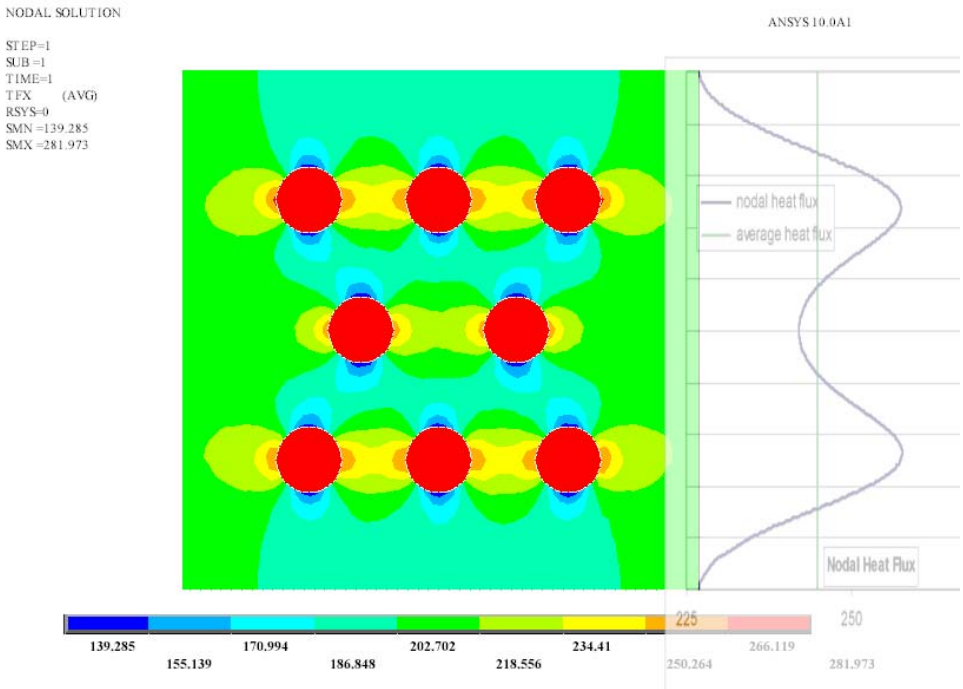

Figure 8. Heat Flux in the *x*-direction. Plate with eight particles evenly spaced, diameter 0.6308 a 10% volume fraction. The superimposed graph shows the nodal values of the heat flux as it varies on the boundary.

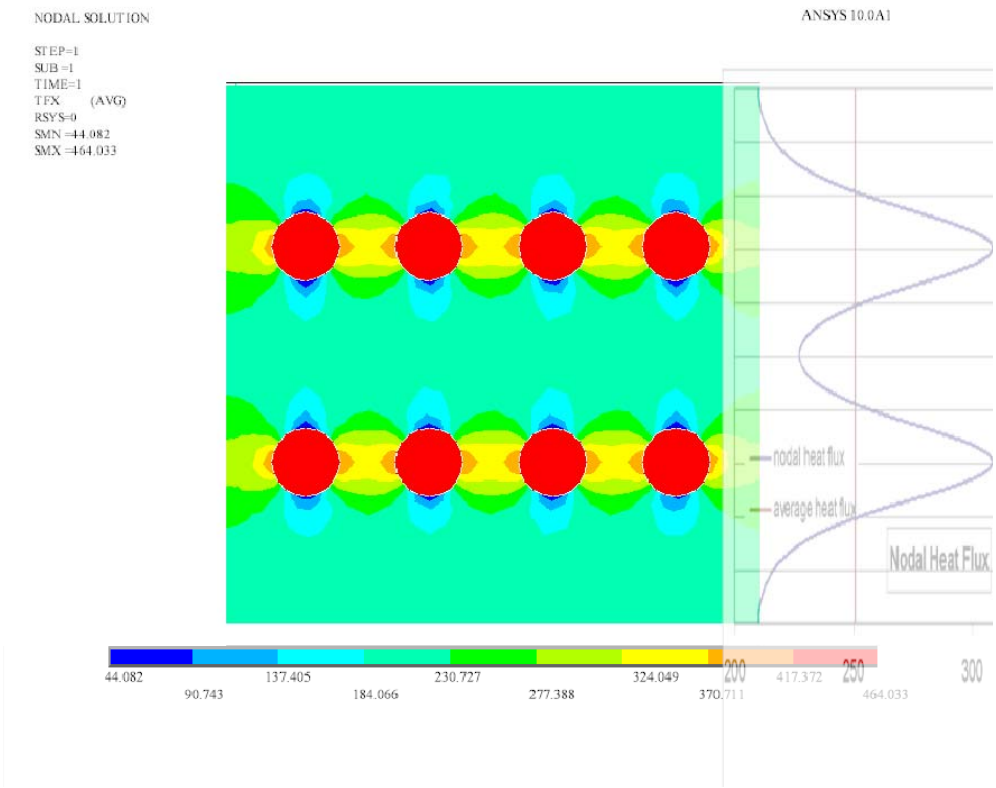

Figure 9. Heat Flux in the x-direction. Plate with eight particles (two rows of four), diameter 0.6308 a 10% volume fraction. The superimposed graph shows the nodal values of the heat flux as it varies on the boundary.

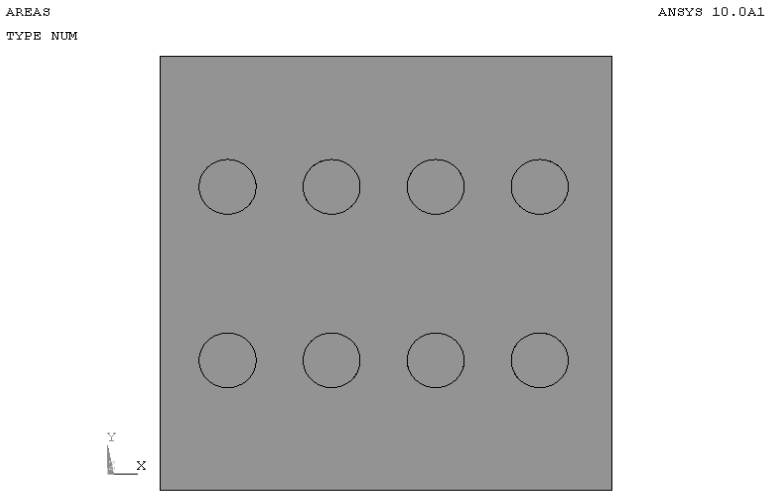

Figure 10. Eight particles (2 rows of 4) diameter 0.6308, a 10% volume fraction. Dimensions of the plate are 5 in the x-direction 5 in the y-direction.

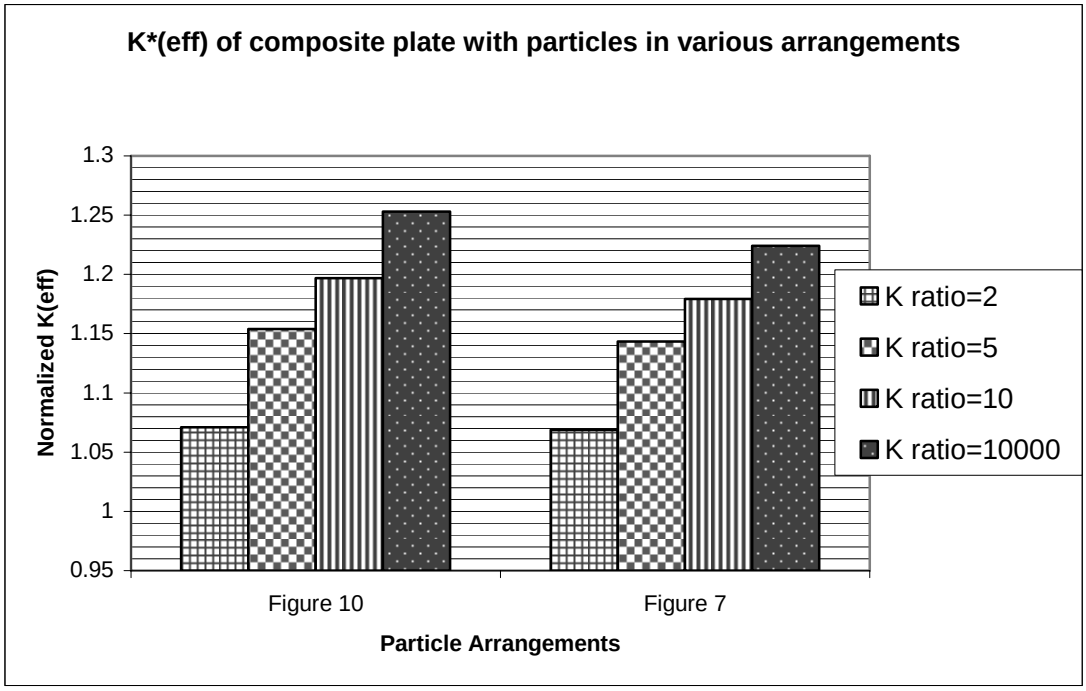

Figure 11. The κ_{eff}^{*} of a plate with 10% volume fraction of a secondary material incorporating Eight particles of diameter 0.6308.

b. Rectangular Strips

The next set of simulations show that a larger number of particle lines of the secondary material, translates into a larger overall κ_{eff} for the plate. Three geometries were compared. Using the 10% volume fraction, the 5x5 plate had horizontal rectangular strips of secondary material running the full width of the plate. The three plates' geometries are:

- A single strip, 0.5 high;
- Five strips, 0.1 high;
- Ten strips, 0.05 high.

Figures 12 and 13 show the results of the three geometries. The data from the κ ratio=10,000 is broken out into a separate graph so that the values in Figure 12 would be discernible with each other. Table 2 list the data for Figures 12 and 13.

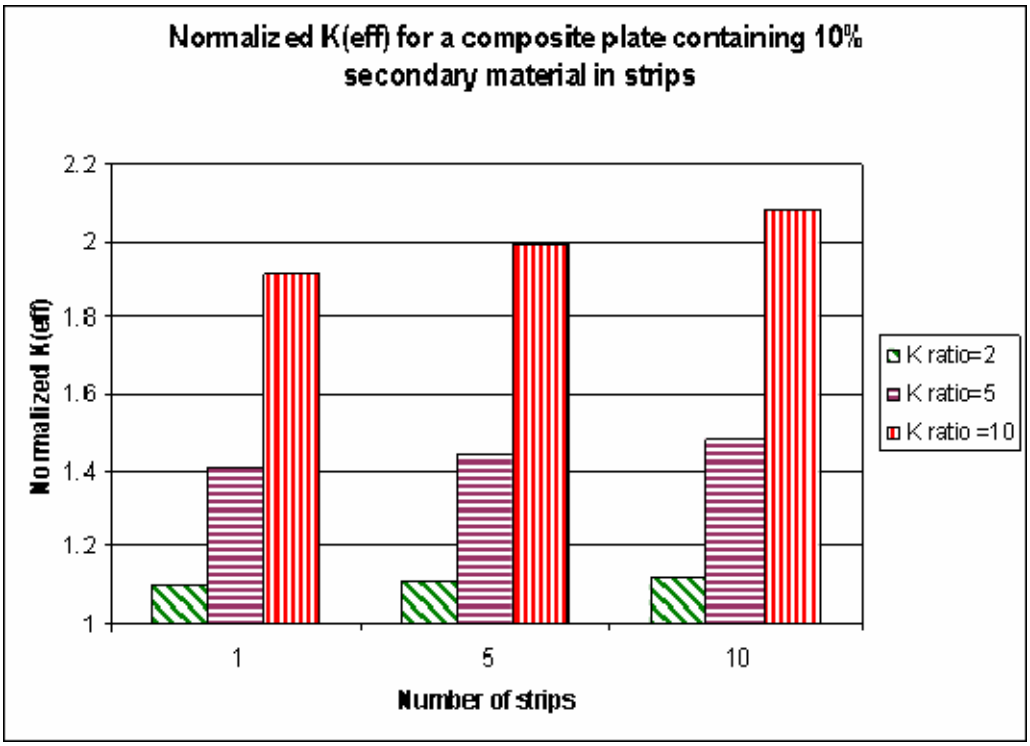

Figure 12. The κ_{eff}^{*} of a plate with a constant 10% volume fraction, in all three cases, of a secondary material in rectangular strips.

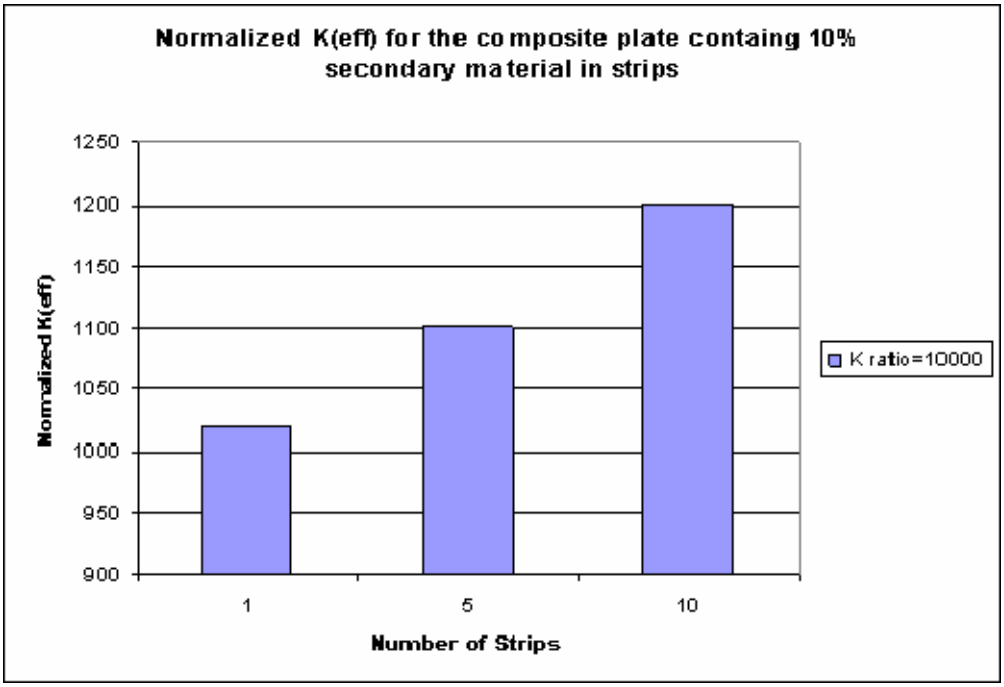

Figure 13. The κ_{eff}^{*} of a plate with a constant 10% volume fraction, in all three cases, of a secondary material in rectangular strips κ ratio=10,000.

K*(eff) values (10%) strips					
number of strips	K ratio =1	K ratio =2	K ratio =5	K ratio =10	K ratio =10000
1	1	1.102	1.408	1.918	1020.898
5	1	1.11	1.44	1.99	1100.89
10	1	1.12	1.48	2.08	1200.88

Table 2. The κ_{eff}^{*} of a plate with a constant 10% volume fraction, in all three cases, of a secondary material in rectangular strips.

c. Ten Percent Discussion

The results of these early models indicate that κ_{eff} is related to the number of horizontal rows of secondary material. More rows of a higher conductive material in the plate created a greater overall heat flux and κ_{eff}^{*}. The size of the particles needs to be reduced to maintain a constant volume fraction and to produce rows of continuity of the secondary material.

3. The 4.7 Percent Volume Fraction Models

Two questions arise from the rectangular strip results. The first is whether the reduction of the particle size truly increases the thermal conductivity of the composite. The other question is, 'what is the importance of the continuity of the secondary material?'. The rectangular geometry for the particles appears to be the ideal case; there is uniform cross section and no breaks in the continuity of the higher thermal conductive material. What is the result when continuity is broken? With these questions the research branched off in two directions. A set of testing to determine what the effects of discontinuity are in the nanocomposite. More specifically how much space between particles can exist and still have a significant increase in κ_{eff}^{*} of the plate. The other separate test looks to verify that smaller particles of a constant volume fraction do actually mean a higher κ_{eff}^{*} for the nanocomposite.

To maintain the constant volume fraction of 4.7% in these models, the dimensions of the composite plate were varied to compensate for the change of the particle size and the addition of spacing between particles.

a. Particle Size Comparisons

This set of comparisons varied the size of the particles and kept the volume fraction and the spacing between particles constant (4.7% and 0.0 respectively), which had the effect of increasing the number of horizontal rows in the composite plate. This tested the idea that the smaller the size of the particle, the greater the effective thermal conductivity of the plate would be. The models for this comparison went through three main evolutions.

(1) Circular Particles Touching Each Boundary with a Single Point. The first evolution modeled the particles as circles, as had been done earlier in the study, and the full circles would be connected in horizontal rows connecting one temperature boundary to the other. (Figure 14) The following geometries were used to compare the effect of the particle size on the thermal conductivity of the plate.

- One row of 5 particles at a normalized diameter of 1
- One row of 7 particles at a normalized diameter of 0.6
- Two rows of 14 particles at a normalized diameter of 0.4
- Three rows of 25 particles at a normalized diameter of 0.2
- Three rows of 50 particles at a normalized diameter of 0.1

The comparison results of these models were inconsistent with the results of the rectangular strip models. The results shown graphically in Figure (15) revealed that there was an upper limit to the enhancement of κ_{eff}^{*}. The limit to the enhancement, even at κ ratios of 10,000, was no more than 50%,. Comparing this to the rectangular models where the thermal conductivity continued to increase at the κ ratio increased, to the order of 100,000%. There appeared to be a problem with this representation of the nanocomposite.

(2) Identifying the Error at the Boundary. The low results were believed to be caused by the particles' single point on the boundaries. The issue was that the plate boundaries contained a point of singularity where the particle intersected the boundary. The point where the higher thermal conductivity of the particle met the boundary that was everywhere else the lower conductivity of the plate, meant that the mesh size on the boundary was insufficient to properly account for this vast change in the nodal heat flux.

The first model to test this theory used the 7 particle geometry from the size testing. One of the particles was split in half, so that a semicircle with the diameter face was on the left and right plate boundaries (Figure 16). The effective thermal conductivity of this geometry had an increase of approximately 200 times that of an isotropic plate at the 10,000 κ ratio, compared to the 50% increase from the previous geometry. This result supported the idea that the comparison results were influenced by the point of singularity.

The next step in identifying the problem, with the circular particles with a point at the boundary, was to develop a hybrid geometry. This model was designed to test the methodology of the work that had been accomplished so far. A plate with six and a half particles where the left boundary had a particle touching at a point and the opposite boundary had the semicircle diameter. The volume fraction for the plate was maintained at 4.7%. The heat flux for both boundaries was calculated showing a significant difference at the two boundaries. At the test κ ratio of 100; the boundary with the half particle had an approximately 125% larger heat flux than did the other temperature boundary. This showed that there was no conservation of heat flux in this geometry, indicating that the model was totally unacceptable for modeling. Similar test, where the geometry was identical on both boundaries (either a single point or a semicircle diameter), did show a conservation of heat flux. The hybrid geometry also showed that the boundaries that included points of singularity were not adequate representations of the nanocomposite.

The conservation of heat flux on symmetric boundaries, and the results from the model with the diameters on the boundaries provided evidence that the circular particle and the testing methodology were valid for the study. Another validation on the process was done, before further testing was accomplished. A plate with a single particle, touching each boundary at a single point was modeled. All of the nodes were identified at the boundaries and 19 interior *x* values. This was done to calculate the heat flux throughout the interior of the plate, and ensure that there was conservation of heat flux throughout the interior of the plate. The results showed that heat flux throughout the interior *x*-values were consistent and at the boundaries the heat flux decreased significantly. This indicated that the process was valid; and continued to validate that the singularity on the boundary was a critical issue.

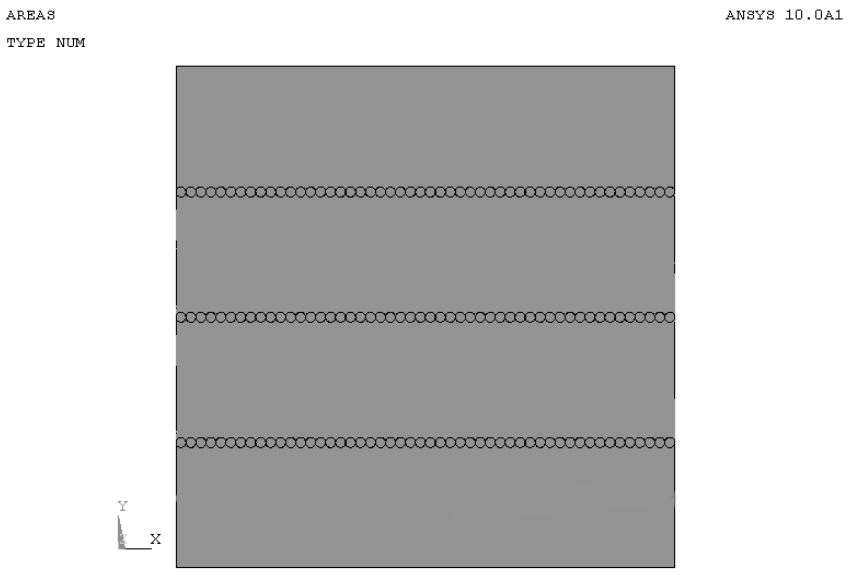

Figure 14. 150 connected circular particles.

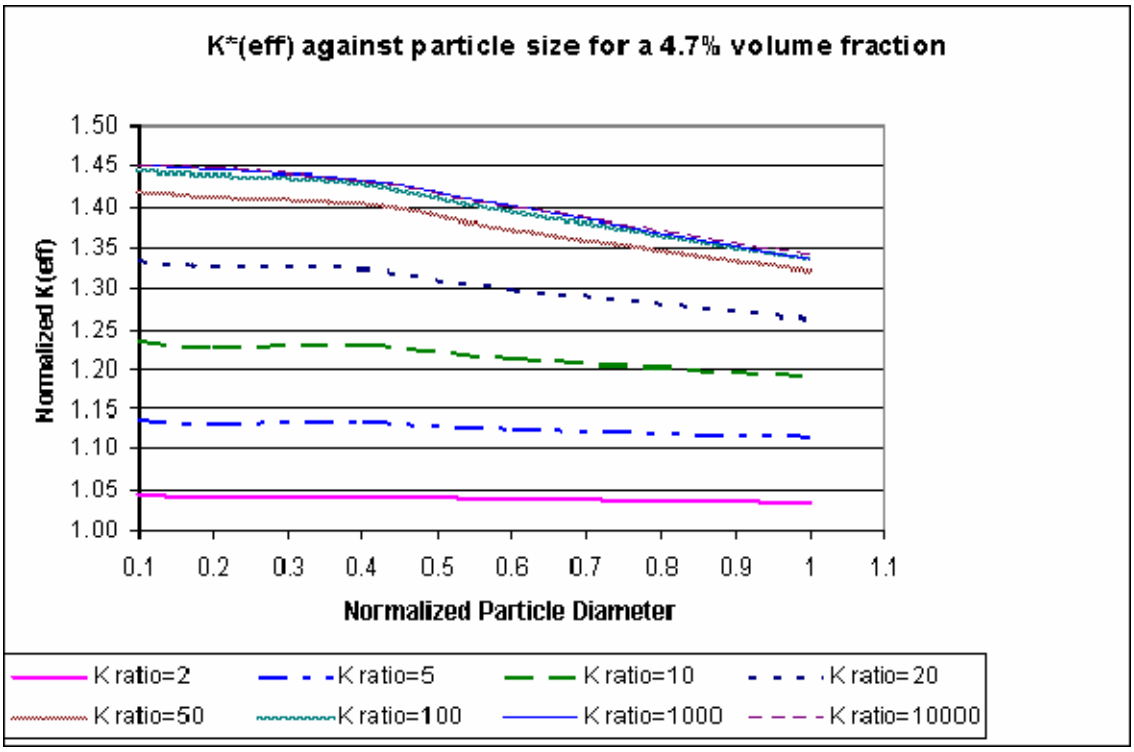

Figure 15. The κ_{eff}^{*} of a plate with 4.7% volume fraction of a secondary material; particles of varying number and diameter; circular particles with points of singularity at the boundaries. Shows that there is an upper limit to the κ_{eff}^{*} which is inconsistent with the earlier models using the rectangular strips.

(3) Circular Particles Touching Each Boundary with a Diameter. The second evolution of the size comparison test used the circular particles of the same size and number that were used for the first evolution, but modified so that a diameter of a circle was on each temperature boundary. Figure (16) is an example of these composite geometries. This modification maintained the particles as circles while eliminating the point of singularity at the boundary. Simulations using this geometry revealed that it also was inconsistent with the results from the ideal case of the rectangular strips. There was not an upper limit to the κ_{eff}^{*} for these geometries, but there was also not any noticeable difference in the κ_{eff}^{*} as the particle size changed (Figure (17)).

The singularity point was also believed to be the issue in this geometry, not at the plate boundaries, but at the point where a particle was in contact with other particles. The mesh near the inter-particle contact point was not able to represent the heat flux in those areas, and thus did not represent the total heat flux of the composite plate. The limitation of the mesh effectiveness was most likely caused by the confined space between the particles and the large difference in the thermal conductivity at the single contact point and the lower heat conductivity of the surrounding material.

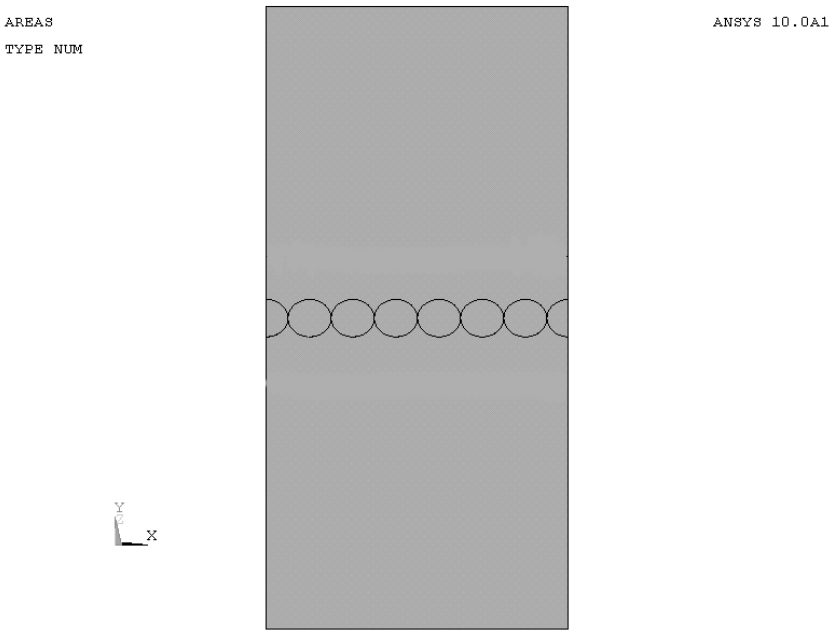

Figure 16. 7 connected circular particles with half particles at the boundaries.

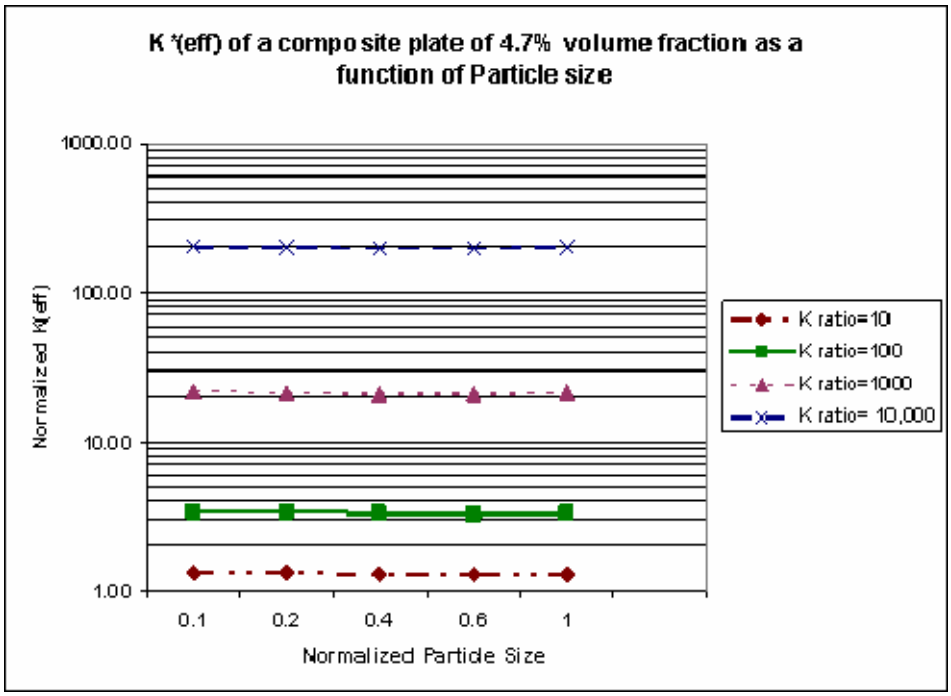

Figure 17. The κ_{eff}^{*} of a plate with 4.7% volume fraction of the secondary material; particles of varying number and size; circle diameter on the boundaries. Does not show any noticeable variation with the change of the particle size. Inconsistent with the rectangular strip models.

(4) Hexagon Shaped Particles. The difference between the geometries of the particles and the rectangular strips is that the strips have a constant cross section of material at every point of the "particle" row. The rows of circular particles only have a singular line of points that are uninterrupted through the length of the plate. To address this issue of single point continuity the shape of the particles were changed to allow more continuity, and more contact area between neighboring particles. The shape picked for the final evolution of the size comparison test was the hexagon. It maintains a significant contact area with the neighboring particles and also has breaks in continuity which represent it more as a particle than the rectangular strips. One face of each particle was in contact with a neighboring particle's face and the opposite face was in contact with a second particle or the plate boundary as illustrated in Figure 18.

The size of the hexagon particles was varied for comparison similarly to the way the circular particles sizes were varied. The κ_{eff}^{*} of the hexagon imbedded plates increased as the κ ratio increased, also similar to the rectangular strips the κ_{eff}^{*} increased as the particle size got smaller translating into more rows of continuity of the secondary material. The comparison between the hexagon particles and rectangular strips is shown in Figure 19, which plots κ_{eff}^{*} of the plate with respect to the normalized particle size. The particle size is normalized with regards to the largest particle of that shape in the study. It shows that κ_{eff}^{*} of the rectangular strips is the most conductive. This was the previous assumption, because of the rectangle had no discontinuity of the secondary material. The rectangular strips geometries do have 0.3% more secondary material, but this alone will not account for the dramatic increase in κ_{eff}^{*}. The hexagon shaped particles follow the same trend as the rectangular strip models, which is the smaller the particle the greater κ_{eff}^{*} of the plate.

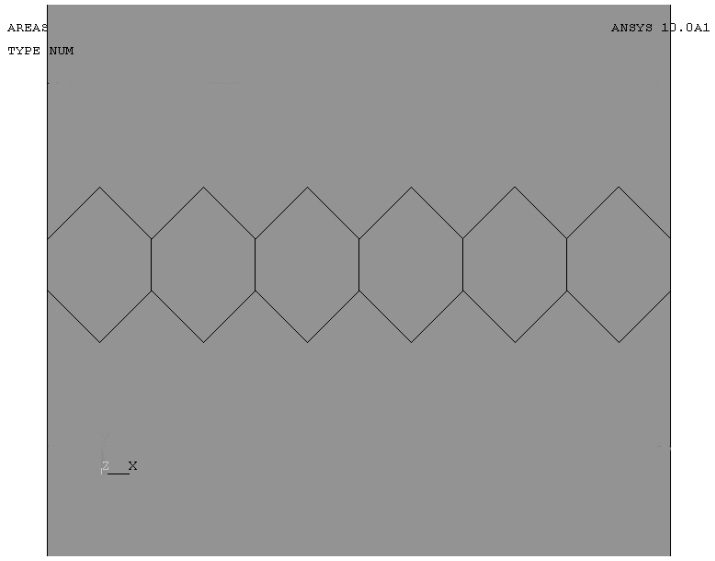

Figure 18. Six Connected hexagonal particles.

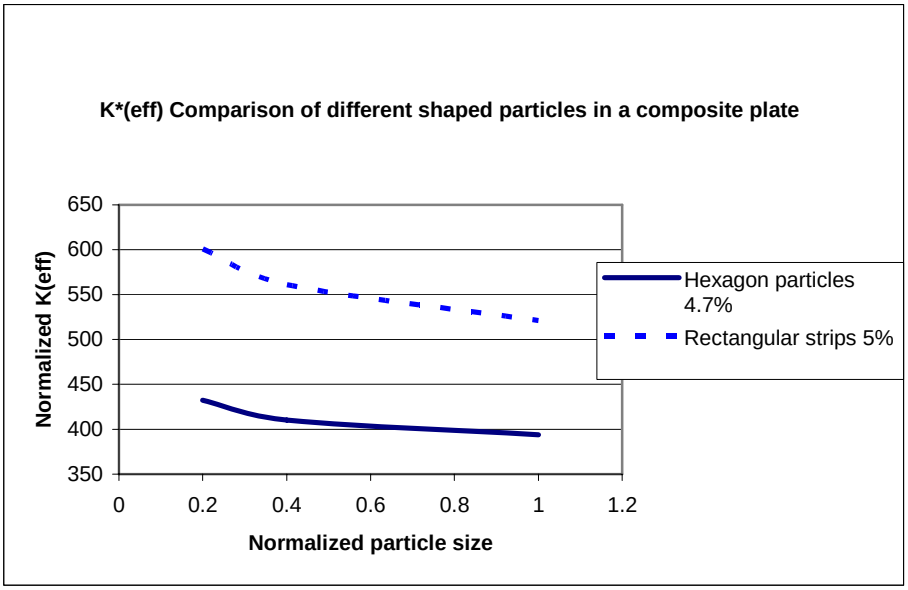

Figure 19. Comparison between particle shapes: rectangle, hexagon and both geometries are at an approximate volume fraction of 4.7%. κ ratio=10,000.

b. Particle Spacing Comparison

(1) Modeling and Setup. The second direction of modeling and simulation was to determine the critical spacing of the secondary particles in regards to the effect on κ_{eff}^{*} of the plate. Staying with the 4.7% volume fraction of the secondary material the initial plate of zero spacing was modeled as a five by five plate with three rows of 50 circular particles, with a diameter of 0.05 units. The dimensions of the plate were altered to maintain the volume fraction as space between the particles increased. The length was function of the particle size and spacing; and the height a function of the length and the volume fraction. The values of the particle spacing were normalized with regard to the radius of the particles: 0.2; 0.4; 1; 1.5; 2; 4; and 8; the κ ratios: 10, 100, 1,000, and 10,000 were used in the simulations.

(2) Shape Error Check. The erroneous results associated with the circular particles were not realized at the time the spacing models were created and tested. Had those results been known the particles would likely

have been shaped as hexagons. As it turns out the only geometry, in the spacing comparison, where the circular particles seem to cause inaccuracies is the geometries of ‘zero’ spacing.

The original particle shape and arrangement for the zero spacing geometry produced inaccurate results as determined in the spacing comparisons as seen in the size comparison using the circular particles. Therefore the results from the hexagon shaped particles (3 rows of 50) were used in place of the erroneous circular geometry for zero spacing. The next question to address was; ‘Do all of the other circular spacing geometries have critical flaws in the calculations?’. The assumption was that circular particles that were spaced apart did not produce bad results, because there were no points of singularity at either the boundaries or between the particles. A check was required, however, before the results could be trusted.

Two geometries of spaced hexagon particles were created; each with three rows of 50 hexagonal particles. They were spaced at the normalized distances of 0.5 and 2; and run at the κ ratio of 100. The κ ratio was picked because in the spacing models higher ratios did not noticeably increase κ_{eff}^{*} of the plate, but there was a large difference from the lower ratios to a ratio of 100. The effective thermal conductivity of the plates with the spaced hexagonal particles was almost identical to that of the circular particles of the same normalized spacing and κ ratio. The hexagon particles actually produced a κ_{eff}^{*} slightly less (although almost negligible) than that of circular particles. This can be explained because circles have a much larger perimeter to area ratio than do hexagons. This means that a larger area is facing each particle for the circle than the hexagon, allowing more continuity for the heat to transfer. These results gave validity that the previously spacing comparison models with circular particles were acceptable and gave accurate results.

(3) Spacing Results and Discussions. Figure 20 indicates the κ_{eff}^{*} values as a function of the normalized spacing value, the associated data in Table 3. The greatest thermal conductivity for the plate occurred when the particles were touching or percolated. The normalized thermal conductivity of the composite became less as the spacing between particles increased. Figure 21 shows a different analysis of the data; what percentage κ_{eff}^{*} of a plate, with secondary particles, is greater than that of an isotropic plate as the spacing between particles increases. This graph is useful, showing what percentage of thermal conductivity enhancement may be expected using the various plate geometries. For example if certain percent increase is needed, Figure 21 can be used to determine the thermal coefficient of the secondary particle and the tolerance of the particle spacing needed to obtain the desired effect.

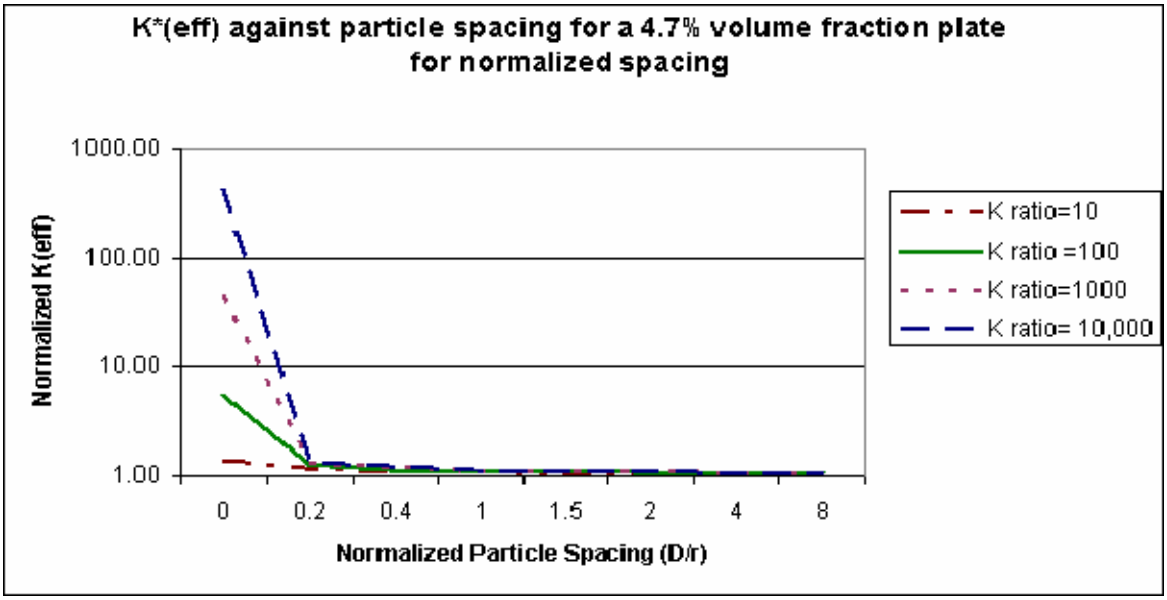

Figure 20. The κ_{eff}^{*} of a plate as the spacing between particles is increased.

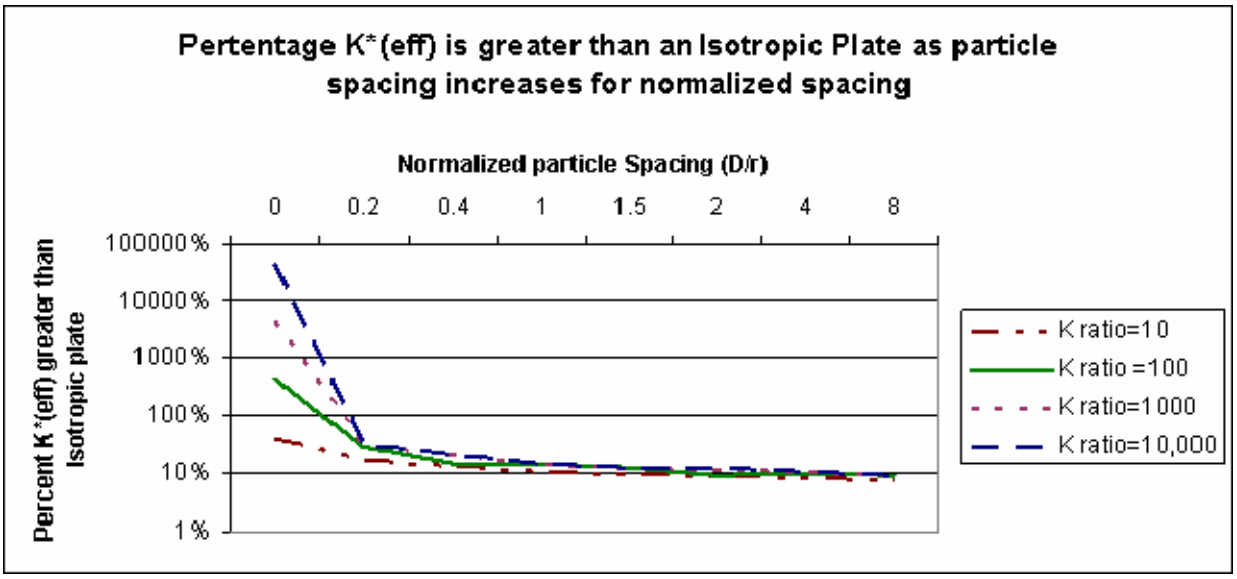

Figure 21. Percentage that κ_{eff}^{*} of a plate with secondary material particles is greater than an isotropic plate as particles are spaced apart.

Normalized K(eff) and Normalized Spacing values (4.7%)					
Spacing (D(spacing)/r(radius))	K=1	k=10	k=100	k=1000	k=10000
0	1	1.395	5.277	44.093	432.254
0.2	1	1.174	1.291	1.309	1.311
0.4	1	1.140	1.149	1.215	1.216
1	1	1.111	1.145	1.150	1.150
1.5	1	1.098	1.125	1.128	1.128
2	1	1.094	1.094	1.118	1.122
4	1	1.084	1.103	1.105	1.105
8	1	1.077	1.093	1.095	1.095

Table 3. The Normalized κ_{eff} as the distance between particles is increased. The particles are circular with the exception of the zero distance those particles are hexagons.

B. MOLECULAR DYNAMICS RESULTS

Each of the four MD models, described as MD Models 1-4 in Chapter II.B, were run with the primary and secondary materials having a constant epsilon value.

The effective *x*-direction heat conductivity for the constant Epsilon calculations is listed in Table 4. Comparing these results to the isotropic

materials, in Figure 22, shows that the addition of the secondary material increases the κ_{eff} of the composite material and that the κ_{eff} of the composite is bound by the κ values of the primary and secondary materials. This gives evidence to the validity of the process.

Geometry	Normalized Effective Thermal Conductivity in the x-direction
Isotropic primary material	1.00
MD Model 3 Continuous section of secondary material (6.02% volume fraction)	27.35
MD Model 4 Continuous section of secondary material (12.04% volume fraction)	35.25
MD Model 1 2 separate sections of secondary material (7.03% volume fraction)	51.79
MD Model 2 2 separate sections of secondary material (14.06% volume fraction)	63.82
Isotropic secondary material	50800.08

Table 4. Heat conductivity of the MD Models with the Constant Epsilon Value=1.

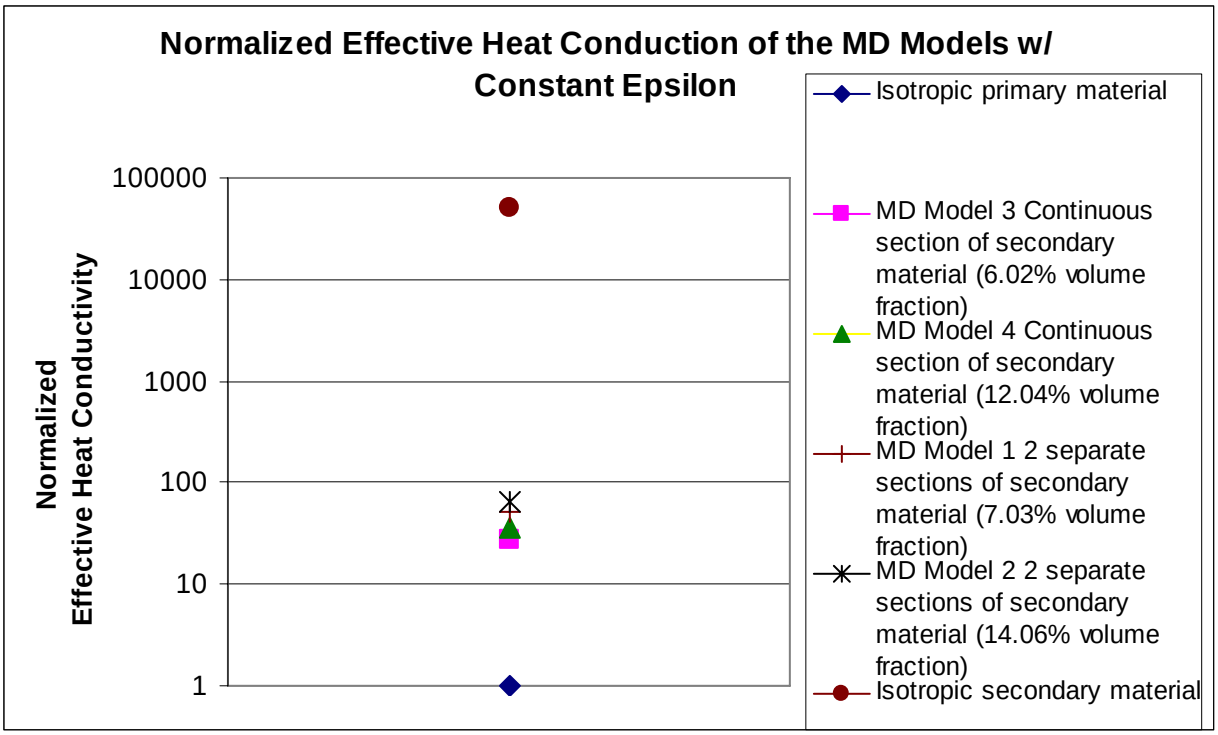

Figure 22. The κ_{eff} of the MD Models with the Constant Epsilon Materials.

The results form the composite materials only are broken out in Figure 23 for an easier comparison. Figure 23 shows that the models with two separate sections of secondary materials have a higher κ_{eff} than do the models with the continuous section of secondary material running the length of the solid. Figure 23 also illustrates that when the respective sections of secondary material are increased and the volume fraction is increased, the κ_{eff} of the composite material also increases which is expected. The unexpected result is that Models 3 and 4 with the continuous section of secondary material have a lower heat conductivity than do Model 1 and 2 with the separated sections; even though the volume fraction of Model 4 is greater than that of Model 1.

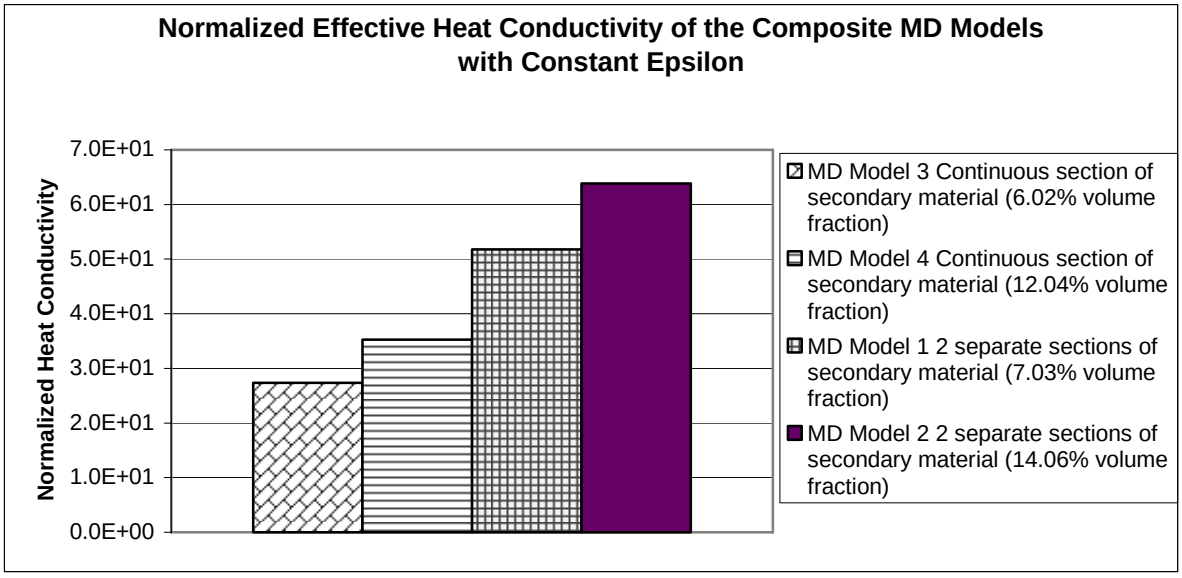

Figure 23. Normalized κ_{eff} of the Nanocomposite MD Models which have Constant Epsilon Valued Materials as the Primary and Secondary Material.

V. CONCLUSIONS

A. CONTINUUM MODEL

The continuum model of the nanocomposite plate showed that the effective thermal conductivity of a material can be significantly improved by the addition of more conductive nanoparticles. This property of the nanocomposite material may be used to assist in the thermal management of any variety of power dense systems (computers, radar, C^4I), allowing heat to be removed from critical areas of the system to increase the reliability and life of the system.

The models also showed that the advantages to using high thermal conductive nanoparticles embedded into a lower thermal conductive material had the intuitive effect of increasing the value of κ_{eff} for the composite material. Another intuitive result is that a larger volume fraction of higher thermally conductive material results in a greater κ_{eff} for the composite.

The more interesting results are associated with the size of the secondary particles and the spacing between them. The results showed that the continuity of the more conductive material, the secondary particles, was the most important factor to increase the κ_{eff} of the composite material. The less discontinuity between particles and the more rows of continuity both equated to higher thermal conductivity of the composite plate. The importance of the continuity was shown by the spacing comparison. The κ_{eff} of the plate decreased significantly as the spacing between particle increased. The particle size comparison illustrated that the more rows of continuity translated into the higher thermal conductivity for the material. To achieve more rows with the same volume fraction the particles' size needed to be smaller. Which can be assumed that the smaller particles imbedded into the material will produce a greater effective thermal conductivity for the material.

This conclusion is important for the future design work in the nano-composites. It shows that if the alignment and orientation of the nanoparticles can be more accurately placed within the composite matrix, the volume fraction may be decreased which will decrease the costs associated with manufacturing the nanoparticles.

The spacing results supplied information about the need for continuity in the secondary material to facilitate a higher κ_{eff}. The greater continuity, or rather the less discontinuity, of the secondary material results in a greater effective thermal conductivity for the composite. The other side of the spacing results is that although the κ_{eff} drops off almost immediately with a slight spacing between particles, there is still significant thermal benefit with the addition of the particles within the composite. This information may also be useful to material designers. A cost analysis can be accomplished using this data to determine how detailed the alignment of particles needs to be in order to meet the thermal requirements of a material. The less stringent the spacing requirement is for the particles, it can be assumed that the cost of manufacturing would decrease.

The other important analysis and results that came from the size comparisons were the modeling limitations using FEM software. The circular shapes of the particles initially were thought to be good representations of the nanoparticles. It appears that the circular particles were better heat conductors than the hexagonal particles. However, the critical flaw in the analysis of the circular particles was the point of singularity.

These results may also help to explain the difficulties associated with experimentally testing the thermal conductivity of nanocomposites. These simulations indicate that continuity of the particles is very important for the thermal conductivity of the nanocomposites. Because of their small size, studies have indicated that the alignment of the CNT and nanoparticles is difficult. If the particles are not aligned or there is discontinuity between the particles it would significantly impact the results of the experimental study.

B FUTURE WORK WITH THE CONTINUUM MODEL

This thesis illustrated that the continuum model is a valid tool for the determination of thermal conduction through nano-composites. Further study may include more accurate representation of the CNT structure. This study looked to represent the CNT as circular and hexagonal particles. Modeling the particles as cylinders or capsule shaped particles may be more informative to the true thermal potential of the CNT-based nanocomposite. The capsule shape has a relatively long axial direction. However, with the addition of the fullerenes at the ends of the tube there is the potential for discontinuities between the CNT, even if they were touching and aligned in the same direction. This capsule shape would be a hybrid of the rectangular strips and circular particles.

With the particles modeled more accurately, the orientation of the particles may be varied to determine if how the thermal conductivity of the composite may be affected by heat flux through the axial direction of the CNT opposed to the radial direction. This may be beneficial in determining the optimal orientation and placement of the CNT throughout the composite material to promote thermal conductivity.

A material designer could use the information: optimized orientation and placement of CNT and values of κ for the CNT and the base materials, to determine the value of κ_{eff} for the composite material. The calculated κ_{eff} can be used to reevaluate the design with regards to the requirements for the material.

C. MOLECULAR DYNAMICS CONCLUSION

The results of the Molecular Dynamics models were consistent with the idea that increasing the volume fraction of the secondary material caused an increase in the effective thermal conductivity for similar geometry composite material. The MD calculations also showed that the thermal conductivity of all of the composite materials fell with in the bounds of the homogenous primary and homogenous secondary materials. Both of these coincide with the results of the Continuum Method.

The results of the Molecular Dynamics calculations, however, do not correspond with all of the conclusions of the continuum calculations. The Continuum Method results show the importance of the continuity of the secondary material through the composite; the MD results actually show that the opposite is true the composites where there is discontinuity had the higher thermal conductivity. It is believed however that the continuum method offers results that are more realistic and that the results from the MD calculations are caused by limitations in the input models. Possible modifications to the model that may improve the MD results are discussed in the next section.

D. MOLECULAR DYNAMICS FUTURE WORK

The initial follow-on study would be to determine the if modifications to the MD model would create results that would confirm the Continuum method results. An area to look at for improvement would be in the number of atoms used for the calculations. The total number of atoms in the materials that were modeled and simulated was relatively small (256). Increasing the number of atoms would provide a larger amount of data for correlation and calculation.

Other areas of potential improvement in the model would be to decrease the *y*-dimension while increasing the x and z dimensions. This would have the effect of creating a thin plate, instead of the cube that was modeled in this study. The dimensional modification would provide more flexibility in the position of the secondary atoms. The thin plate model would also be a closer comparison to the continuum model plate.

The MD models may, in the further studies, better represent the nanoparticles with in the FCC structure Similar to the Continuum Model, the MD work may be improved by incorporating more accurate representations of the Carbon Nanotubes within the nanocomposite. The molecular dynamics model of a SWNT has previously been developed and the FCC structure was used in this thesis. The challenge would be to incorporate the SWNT model with into the FCC model. Testing and research would be needed to determine the acceptable lattice distances of the FCC structure adjacent to the SWNT and at locations far

from it, and the associated Sigma and Epsilon values for the SWNT, the FCC structure, and the atomic positions of interaction between the FCC and the SWNT.

The difficulty is in the computational time required for these calculations. It is non-linear relationships between the number of atomic positions and the computational time required for MD calculations. More atoms and a greater the degree of complexity in the system equate to a much greater need for computing power.

THIS PAGE INTENTIONALLY LEFT BLANK

LIST OF REFERENCES

1. Qian, D., Dickey, E.C., Andrews, R., Rantell, T. (2000). Load transfer and deformation mechanisms in carbon nanotube-polystryene composites. *Applied Physics Letters*, *76*, 2868-2870.

2. Iimiji, S. (1991). Helical microtubes of graphitic carbon. *Nature, 354,* 56-58.

3. Hone, J., Whitney, M., Zettl, A. (1999).Thermal conductivity of single-walled carbon nanotubes. *Synthetic Metals, 103,* 2498-2499.

4. Hanson, T. (September 13, 2004). *Laboratory grows world record length carbon nanotube.* Retrieved May 10, 2007 from http://www.lanl.gov/news/index.php/fuseaction/home.story/story_id/2195.

5. Kaye, G.W.C, Laby, T.H., *Tables of Physical and Chemical Constants*, 13th ed., 1966.

6. Thorstenson, E.T., Zhifeng, R., Chou T. W. (2001) Advances in the science and technology of carbon nanotubes and their composites: a review. *Composites Science and Technology*, 61, 1899-1912.

7. Hone, J., Whitney, M., Zettl, A. (1999).Thermal conductivity of single-walled carbon nanotubes. *Synthetic Metals, 103,* 2498-2499.

8. Hone, J., Whitney, M., Piskoti, C., Zettl, A. (1999).Thermal conductivity of single-walled carbon nanotubes. *Physical Review B*, 59, 2514.

9. Che, J., Cagin, T., Goddart, W. A. III, (9 September 1999). "Thermal conductivity of carbon nanotubes." *Nanotechnology, Seventh Foresight Conference on Molecular Nanotechnology*. Retrieved May 14, 2007 http://www.wag.caltech.edu/foresight/papers/Che99/.

10. Berber, S., Kwon, Y-K., Tomanek, D., (2000). Unusually High Thermal Conductivity of Carbon Nanotubes, *Physical Review Letters 84,* 4613-4616.

11. Choi, S.U.S., Zhang, Z.G., Yu, W., Lockwood, F.E., Grulke, E.A. (2001). Anomalous thermal conductivity enhancement in nanotube suspensions. *Applied Physics Letters*, *79*, 2252-2254.

12. Biercuk, M.J., Llaguno, M.C., Radosavljevic, M., Hyun, J.K., Johnson, A.T., Fischer J.E. (2002). Carbon nanotube composites for thermal management. *Applied Physics Letters, 80*, 2767-2769.

13. Nan, C.-W., Shi, Z., Lin, Y. (2003). A simple model for thermal conductivity of carbon nanotube-based composites. *Chemical Physics Letters*, *375*, 666-669.

14. Nan, C.-W., Shi, Z., Lin Y. (2003). A simple model for thermal conductivity of carbon nanotube-based composites. *Chemical Physics Letters*, 375, 668.

15. Liu, Y.J., Chen, X.L. (2003). Continuum Models of Carbon Nanotube-Based Composites Using the Boundary Element Method. *Electronic Journal of Boundary Elements, 1*, 316-335.

16. Oh, J.J, *Determination of Young's Modulus of the Carbon Nanotube using MD Simulations*, Master's Thesis, Naval Postgraduate School, Monterey, California, December 2003.

17. Haile, J.M., *Molecular Dynamics Simulation Elementary Methods.* New York, NY: John Wiley and Sons, Inc. 1997.

18. Incropera, F. P., David P. DeWitt. Introduction to Heat Transfer. New York, NY: John Wiley and Sons, Inc. 2002.

19. Kim, P., Shi, L., Majumdar, A., McEuen, P.L. *(2001)*. Thermal Transport Measurements of Individual Multiwalled Nanotubes. *Physical Review Letters, 87, 215502*.

20. Kwon, Y. (2006) MATLAB code modified to solve the thermal conduction problem. Based on FORTRAN *mdss* by Haile, J.M. (1992).

21. Kwon, Y. (2006) MATLAB code modified to solve the thermal conduction problem. Based on FORTRAN *ssfcc* by Haile, J.M. (1992).

INITIAL DISTRIBUTION LIST

1. Defense Technical Information Center
   Ft. Belvoir, Virginia

2. Dudley Knox Library
   Naval Postgraduate School
   Monterey, California

3. Young Kwon
   Naval Postgraduate School
   Monterey, California

4. Daniel Kidd
   Naval Postgraduate School
   Monterey, California